



KADIR HAS UNIVERSITY
SCHOOL OF GRADUATE STUDIES
DEPARTMENT OF COMPUTATIONAL BIOLOGY AND BIOINFORMATICS

**REPURPOSING OF EXISTING DRUGS FOR
TREATMENT OF COVID-19 TARGET RNA-DEPENDENT
RNA POLYMERASE (RdRp) ENZYME-USING IN SILICO
SCREENING TECHNIQUES**

MELTEM YILDIRIM

MASTER'S DEGREE THESIS

İSTANBUL, DECEMBER, 2021

Meltem Yildirim	Master's Degree Thesis	2021
-----------------	------------------------	------

Student' s Full Name

Ph.D. (or M.S. or M.A.) Thesis

2011

**REPURPOSING OF EXISTING DRUGS FOR
TREATMENT OF COVID-19 TARGET RNA-DEPENDENT
RNA POLYMERASE (RdRp) ENZYME-USING IN SILICO
SCREENING TECHNIQUES**

MELTEM YILDIRIM

MASTER of SCIENCETHESIS

Master Degree Thesis submitted to the School of Graduate Studies with the aim to meet the partial requirements required to receive a Master's Degree in the department of Computational Biology and Bioinformatics.

İstanbul, December 2021

DECLARATION ON RESEARCH ETHICS AND PUBLISHING METHODS

I, MELTEM YILDIRIM; hereby declare

- that this Master of Science Thesis that I have submitted is entirely my own work and I have cited and referenced all material and results that are not my own in accordance with the rules;
- that this Master of Science Thesis does not contain any material from any research submitted or accepted to obtain a degree or diploma at another educational institution;
- and that I commit and undertake to follow the "Kadir Has University Academic Codes of Conduct" prepared in accordance with the "Higher Education Council Codes of Conduct".

In addition, I acknowledge that any claim of irregularity that may arise in relation to this work will result in a disciplinary action in accordance with the university legislation.

MELTEM YILDIRIM

29.12.2021

APPROVAL

This thesis, titled REPORPUSING OF EXISTING DRUGS FOR TREATMENT OF COVID-19 TARGET RNA-DEPENDENDT RNA POLYMERASE (RdRp) ENZYME USING IN SILICO SCREENING TECHNIQUES submitted by MELTEM YILDIRIM, in partial fulfillment of the requirements for the degree of Master of Science in Computational Biology and Bioinformatic is approved by

Prof. Dr. Kemal YELEKÇİ (Advisor)

.....

Kadir Has University

Assoc. Prof., Bengü Özüğur UYSAL

.....

Kadir Has University

Prof. Dr, Safiye ERDEM

.....

Maramara University

I confirm that the signatures above belong to the aforementioned faculty members.

Prof. Dr. Mehmet Timur AYDEMİR

Director of the School of Graduate Studies

APPROVAL DATE: 13.01.2022

Dedicated to My Parents ...

ACKNOWLEDGEMENT

First of all, Head of Bioinformatics and Genetics Department Prof. Kemal Yelekçi Thank you very much for taking the time to answer all my questions and problems sincerely. It was a unique opportunity to have the opportunity to work with him over the years.

I am grateful to Zuhâl Aydın Tanyeri and Deniz Caliskan for their patience and support in overcoming the numerous obstacles we encountered throughout my research. I would like to thank my dear friends İlayda Nur Ünal and Nurdeniz Nalbat, who helped me with the lack of knowledge and program I experienced, for not leaving me alone.

I would like to thank all our faculty members who shared their experiences and knowledge with me from the beginning to the end.

I would like to express my endless gratitude to Nazmina Mert, who helped me with my knowledge deficiencies in completing my thesis and I would like to say that I am grateful.

Finally, I would like to thank my family for their support and Yakup Kılıç, Şule Derya for always motivating me.

This thesis I wrote and the graduate program I will complete; I present to my dear cousin Özgül Kerimoğlu, Who is no longer with us.

REPURPOSING OF EXISTING DRUGS FOR TREATMENT OF COVID-19
TARGET RNA-DEPENDENT RNA POLYMERASE (RdRp) ENZYME-USING IN
SILICO SCREENING TECHNIQUES

ABSTRACT

Coronavirus is a disease that has killed more than 5 million people worldwide since 2019. Corona, which has made its name among the diseases that constitute a pandemic by the world health organization in 2020, is observed as a severe common upper respiratory infection. While the symptoms of the disease show themselves after 5-6 days, their severity starts to show after these days. The virus settles in the respiratory tract and destroys healthy alveoli and surrounding cells. An active and effective method has not yet been found in the treatment of the coronavirus. This study, it is aimed to create a drug form to be used for the loss and slowing of the effect of the virus. It is known that if the mechanism of RNA-dependent RNA polymerase or RNA replicase enzyme, which plays an effective role in the reproduction mechanism of the virus, is blocked, the virus reproduction rate slows down and loses its effect. In our study, a 7bv2 (Pdb format) enzyme-containing Remdesivir (one of the common drugs used for the treatment of the disease) and 6m71 (Pdb format) enzyme, as well as SARS-CoV-2 Helicase Targeted Library from OTAVA chemicals were used. To produce two enzyme inhibitors, it is aimed to obtain the best energy value by subjecting the molecules in the database with different precision values to the docking process. After this process, the drug properties of the chemicals will be evaluated by using ADME applications on the complex structure formed. As a final control of the processes, it will be subjected to the NAMD process to see the potential energy and other important properties of the complex structure created.

Keywords: Coronavirus, RdRp, Docking, in-silico-screening, Molecular Simulation, ADME

COVID-19 HEDEF RNA BAĞIMLI RNA POLİMERAZ (RdRP) ENZİMLERİNİN
TEDAVİ İÇİN MEVCUT İLAÇLARIN YENİDEN KULLANILMASI SİLİKO
TARAMA TEKNİKLERİNDE KULLANILMASI

ÖZET

Korona virüsü 2019'dan bu yana dünya genelinde 5 milyondan fazla insanın hayatını kaybetmesine neden olan hastalıktır. 2020 yılında dünya sağlık örgütü tarafından pandemi oluşturan hastalıklar arasına adını yazdıran korona şiddetli yaygın üst solunum enfeksiyonu olarak gözlemlenmektedir. Hastalığın belirtileri 5-6 gün sonra kendini gösterirken şiddetini de bu günlerden sonra göstermeye başlamaktadır. Virüs solunum yollarına yerleşerek sağlıklı alveolleri ve çevresindeki hücreleri tahribata uğratmaktadır. Korona virüs tedaisinde henüz aktif ve etkili yöntem bulunamamıştır. Bu çalışmada da virüsün etkisinin yitirilmesi ve yavaşlatılmasıyla ilgili kullanılacak bir ilaç formu oluşturmak hedeflenmektedir. Virüsün üreme mekanizmasında etkili rol oynayan RNA'ya bağımlı RNA polimeraz veya RNA replikaz enziminin mekanizması bloke edilirse virüs üreme hızının yavaşladığı ve etkisini yitirdiği bilinmektedir. Çalışmamızda Remdesivir (hastalığın tedavisi için kullanılan yaygın ilaçlardan) içerikli bir 7bv2 (Pdb format) enzimi ve 6m71 (Pdb format) enziminin yanında OTAVA chemiacals'dan alınan 'SARS-CoV-2 Helikaz Hedefli Kitaplığı' kullanılmıştır. İki enzim inhibitör üretmek amaçlı veri bankasındaki moleküllerde farklı kesinlik değeri içeren uygulamalarda yerleştirme/kenetleme işlemine tabi tutularak en iyi enerji değerinin elde edilmesi hedeflenmiştir. Bu işlemin ardından oluşturulan kimyasal yapı üzerinde ADME uygulamaları kullanarak kompleksin ilaç olabilme özellikleri değerlendirilecektir. Yapılan işlemlerin son kontrolü olarak ise oluşturulan kompleks yapının potansiyel enerjisini ve diğer önemli özelliklerini görmek için NAMD işlemine tabi tutulacaktır.

Anahtar Sözcükler: Koronavirüs, RdRp, Docking(yerleştirme), in-sliko tarama, Moleküler Simulasyon, ADME

TABLE OF CONTENTS

ACKNOWLEDGEMENT	iii
ABSTRACT	iv
ÖZET	v
LIST OF FIGURES	viii
LIST OF TABLES	ix
LIST OF ICONS	x
LIST OF ABBREVIATIONS	xi
1. INTRODUCTION	1
1.1 COVID-19's Mode of Action	1
1.2 Virulence Factors of COVID-19	4
1.3 Symptoms of Covid-19	5
1.4 Diagnosis	6
1.5 Treatments	6
1.6 RNA-dependent RNA polymerases (RdRp)	8
1.7 Ligand-Based Drug Design	8
2. MATERIALS AND METHODS	9
2.1 Protein Preparation	9
2.2 Ligand Preparation	15
2.3 Docking Process	16
2.4 ADMET Property Prediction	22
2.5 Preparation of 2D and 3D interaction maps of Ligands with Macromolecule	24
2.6 Molecular Dynamics Simulation Application using NAMD	25
3. RESULTS	26
3.1 PyRx Autodock-Vina Results	26
3.2 Autodock4 Results	28
3.3 ADMET Application Results	29
3.4 2D and 3D Diagram Results	32
3.5 NAMD Molecular Dynamic Simulation Results	35
3.5.1 Root Mean Square Deviation (RMSD)	35

3.5.2 Root Mean Square Fluctuation (RMSF)	36
3.5.3 Radius of Gyration (Rg)	37
3.5.4 Potential Energy (PE)	38
4. CONCLUSION	39
REFERENCES	40

LIST OF FIGURES

Figure 1-1-1 Genome representation of Covid-19 virus(Boopathi, Poma and Kolandaivel, 2020).	2
Figure 1-1-2 Detailed picture of Covid-19 virus. (Boopathi, Poma, and Kolandaivel, 2020).	3
Figure 1-1-3 Mechanism of COVID-19 entry and viral replication and viral RNA packing in the human cell. (Boopathi, Poma, and Kolandaivel, 2020).	4
Figure 1-2-1 COVID-19 infection in the lungs at various stages(Kumar et al., 2021).	5
Figure 1-5-1 Remdesivir mode of action. (invivogen.com, n.d.)	7
Figure 2-1-2 Ligand and activator information of 7bv2.	10
Figure 2-1-3 Discovery Studio information of 7bv2.pdb.	11
Figure 2-1-4 7bv2's ligand coordinates were found using the sphere.	11
Figure 2-1-5 Preparation of macromolecule 7bv2.	12
Figure 2-1-6 Energy minimization (clean geometry) process.	13
Figure 2-1-7 Discovery Studio information of 6m71.pdb	14
Figure 2-1-8 Protein groups information of 6m71.pdb	14
Figure 2-1-9 Energy minimization (clean geometry) process.	15
Figure 2-2-1 Example of ligand compounds with NSP13 produced using molecular docking. (OTAVA chemicals, n.d.)	16
Figure 2-3-1 The start of docking preparations in Autodock Tools.	18
Figure 2-3-2 Saving the ligand in .pdbqt format.	18
Figure 2-3-3 Uploading macromolecules to Autodock tools.	19
Figure 2-3-4 Grid parameters of 6m71 enzyme.	20
Figure 2-3-5 Lamarchian Genetic algorithm values.	21
Figure 3-4-1 2D and 3D images of compound 7bv2 and its original ligand (F86).	32
Figure 3-4-2 2D and 3D image of compound 7bv2 and Molecule1078(ligand).	33
Figure 3-4-3-18 2D and 3D images of compounds 6m71 and Molecule618(ligand).	34
Figure 3-5-1 RMSD graphs of 7bv2 and Molecule1078 complex.	36
Figure 3-5-2 RMSF graphs of 7bv2 and Molecule1078 complex.	37
Figure 3-5-3 Rg graph of 7bv2 and Molecule1078 complex.	37
Figure 3-5-4Potential Energy graph of 7bv2 and Molecule1078 complex.	38

LIST OF TABLES

Table3-1-1 Top 20 binding affinity energies of 6m71.pdb enzyme docked using PyRx-Autodock-Vina.	26
Table 3-1-2 Top 20 binding affinity energies of 7bv2.pdb enzyme docked using PyRx-Autodock-Vina.	27
Table 3-2-1 Binding energy values of the best 5 compounds according to Autodock4 for 6m71.	28
Table 3-2-2 Binding energy values of the best 5 compounds according to Autodock4 for 7bv2.	28
Table 3-3-1 SwissAdme ADME properties.	29

LIST OF ICONS

Å	Angstrom
K	Kelvin
%	Percentage
σ	Sigma
π	Pi
α	Alpha
B	Beta
γ	Gama
δ	Delta

LIST OF ABBREVIATIONS

2D: 2 Dimensional

3D: 3 Dimensional

ACE2: Angiotensin-converting enzyme 2

ADMET: Absorption, Distribution, Metabolism, Elimination, and Toxicity

ADT: AutoDockTool

AMBER: Assisted Model Building with Energy Refinement

ARDS: Acute Respiratory Distress Syndrome

BBB: Blood-Brain Barrier

COVID-19: Coronavirus Disease of 2019

Dsv: Discovery Studio Visualizer

ER: Endoplasmic Reticulum

HBA: Hydrogen Bond Acceptor

HBD: Hydrogen Bond Donor

HE: Hemagglutinin-esterase

LogP: Partition Coefficient

LogS: Aquetenius Solubility

MD: Molecular Dynamic

MERS-CoV: Middleeast respiratory syndrome coronavirus

Mg: Magnesium

Mw: Molecular Weight

NaCl: Sodium Chloride

NAMD: Nanoscale Molecular Dynamics

nRot: Number of Rotatable Bonds

Pdb: Protein Data Bank

POP: PYROPHOSPHATE 2-

RCSB: Research Collaboratory for Structural Bioinformatics

RdRP: RNA-dependent RNA polymerase

Rg: Radius of Gyration

RMSD: Root Mean Square Deviation

RMSF: Root Mean Square Fluctuation

RNA: Ribonucleic Acid

RTC: Replication transcription complex

RTP: Triphosphate form of Remdesivir

SARS-CoV: Severe acute respiratory syndrome coronavirus

SARS-CoV-2: Severe acute respiratory syndrome coronavirus 2

SIRS: Systemic inflammatory response syndrome

TPSA: Topological polar surface area

WHO: World Health Organization

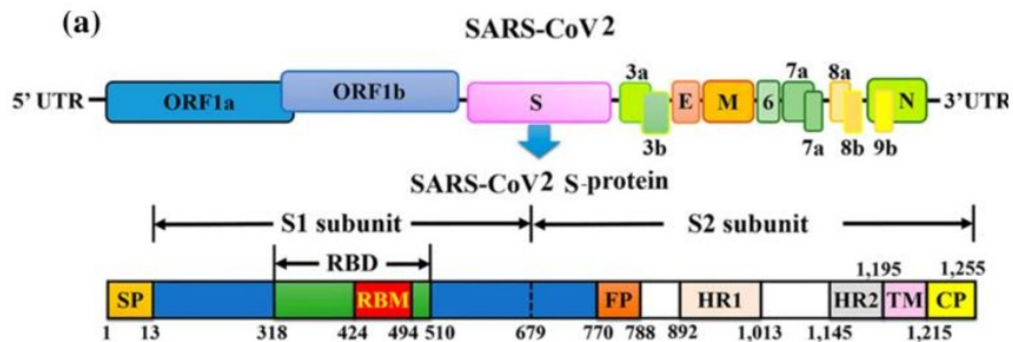
Zn: Zinc

1. INTRODUCTION

Corona Virus Disease 2019 (COVID-19) is a global pandemic caused by a novel coronavirus that first appeared in December 2019(Gao et al., 2020). It is a crisis-causing situation that resulted in more than 270,319,171 million infections and 5,321,218 deaths reported in February 2020, with these numbers still uncontrollable (Worldometer, 2021). It was announced by the World Health Organization (WHO) that the outbreak of COVID-19 on March 11, 2020, following an uncontrollable number of diseases and deaths, gained a dimension as the number of diseases originating in China and deaths continued to increase internationally (WHO, 2020) declared a pandemic disease (World Health Organization, 2019). Until March 19, 2020, no organization or community announced that this disease has gained or will become a pandemic. The information that the disease first started in Wuhan, China, and that it originated from a market where consumed bats and similar animals were sold, and the consumption of these animals spread from mouth to mouth. With the statement made by the World Health Organization, it was scientifically explained that the coronavirus is genetically very similar to the bat (World Health Organization, 2019). All other societies argued that animals such as bats, pangolins, pigs, and weasels, raccoons were linked to the event that they carried this virus. (Carver and Phillips, 2020)(Chu et al., 2020a). Coronaviruss are divided into four genera (α , β , γ , and δ), and they have been found in a wide range of animal species, including humans(Chu et al., 2020b). It is known that SARS-Cov-2 taxonomically belongs to the Sarbecovirus subgenus of the family of coronaviruses, which includes more than one species that causes humans to have the disease from mild to severe. SARS-CoV-2 is a novel coronavirus that has been reported to infect humans after MERS-CoV is the most known progenitor strain, SARS-CoV(Yüce, Filiztekin, and Özkaya, 2021). Coronavirus is a member of the similar virus family with MERS and SARS, and it shows effects such as colds, severe acute respiratory syndrome, which have similar symptoms to them

1.1 COVID-19's Mode of Action

It is known that the coronavirus genome consists of about 30000 nucleotides and also consists of four structural proteins. These are: 1. Nucleocapsid (N) protein, 2. Membrane (M) protein, 3. Spike (S) protein, and 4. Envelope (E) protein and several non-structural proteins (nsp) were shared as codes (*Figure 1-1-1*). It is known that inside the protein coat, there are nuclear capsid or N-proteins attached to the single positive-stranded RNA of the virus.



The S protein is consisting of the S1 and S2 subunits. The S1/S2 cleavage sites are highlighted by dotted lines. In the S-protein, cytoplasm domain (CP); fusion peptide (FP); heptad repeat (HR); receptor-binding domain (RBD); signal peptide (SP); transmembrane domain (TM) are shown

Figure 1-1-1 Genome representation of Covid-19 virus(Boopathi, Poma and Kolandaivel, 2020).

The job of the N protein is to coat the viral RNA genome, which plays a vital role in its replication and transcription. The most abundant protein on the viral surface is the M protein. This protein is said to be the regulator of the virus. S proteins are located on the virus surface and help the virus to bind to receptors. Protein E, on the other hand, is a small membrane protein consisting of a small number of amino acids (76-109) (Kirchdoerfer et al., 2016). There is also a Hemagglutinin-esterase dimer (HE) protein on the surface. It is a protein that is not needed for virus replication. You can see all of these proteins and structures mentioned in *Figure 1-1-2*.

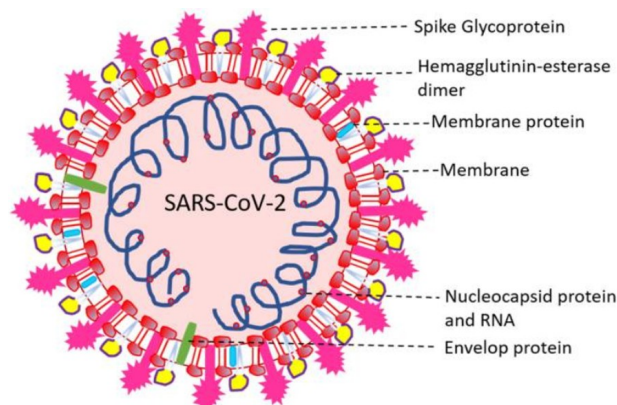


Figure 1-1-2 Detailed picture of Covid-19 virus. (Boopathi, Poma, and Kolandaivel, 2020).

The S protein interacts with ACE2 receptors in the lungs, allowing the virus to enter. S1 and S2 are two components of the coronavirus S protein. The fusion peptide is released when the S2 domain is cleaved. As a result of this occurrence, the membrane fusion process will activate. Following these events, the virus enters the endocytosis process. The membrane fusion mechanism within the endosomes is activated after they enter the cytoplasm. The virus is released into the cytoplasm when the endosome opens (Boopathi, Poma, and Kolandaivel, 2020). The ability to hydrolyze endogenous proteins is enabled by the opening of the viral envelope (N). Spike, host proteases, break the S1 subunit once it interacts with a receptor on the surface of the target host cell. Fusion is likely to occur thanks to the S2 subunit (Simmons et al., 2005). The single-stranded RNA fragment carrying the viral genetic information is released into the cytoplasm as the final step in these processes. The enzyme RNA-dependent RNA polymerase produces negative sense RNA when it replicates positive-sense RNA. Negative sense RNA is transcribed, or positive sense RNAs are transcribed from negative-sense RNA (included in the viral genome). Viral proteins such as spike, membrane, envelope, and nucleocapsid can be produced by translating transcribed mRNAs (Kumar et al., 2021). Replication and transcription processes occur through the replication/transcription complex (RTC). This complex is encoded in the viral genome and consists of non-structural proteins (nsp). Following the positive RNA genome, the open reading frame ORF replicase is set to work to produce proteins (van Hemert et al., 2008). These proteins use the genome as a beacon to create RNAs. M, S, and E, the structural viral proteins, are made in the cytoplasm before being introduced into the endoplasmic reticulum (ER) (**Figure1-1-3**), and transfer to the endoplasmic reticulum Golgi intermediate chamber is performed. Final attachments are made to support viral activity and they are taken out of the cell by the process of exocytosis (Boopathi, Poma and Kolandaivel, 2020).

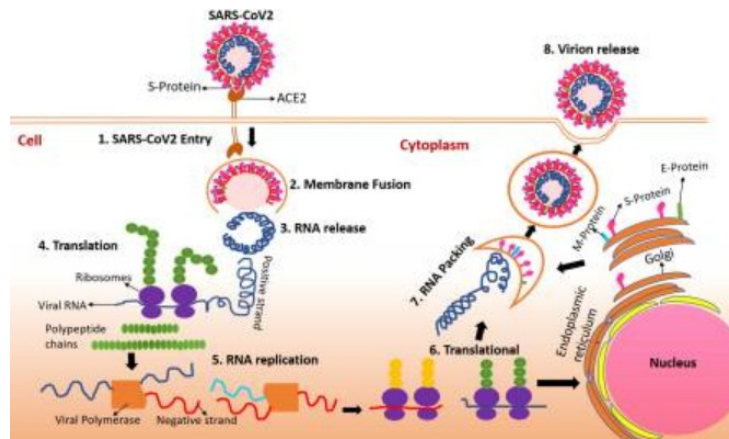


Figure 1-1-3 Mechanism of COVID-19 entry and viral replication and viral RNA packing in the human cell. (Boopathi, Poma, and Kolandaivel, 2020).

1.2 Virulence Factors of COVID-19

Researchers generally presented the symptoms of the disease in three stages. The first stage is the time to be a carrier without showing symptoms for 1 to 2 days after being infected. At this stage, the virus binds to the Angiotensin-converting enzyme 2 (ACE-2) receptors and multiplies. At this stage, there is information that the virus will be detected using the swab test. The second stage is the upper respiratory tract infection stage, where the virus migrates down after settling in the respiratory tract. The majority of infected patients have an upper respiratory tract infection. The final phase is the acute respiratory distress syndrome (ARDS) and Hypoxia phase, where the virus reaches and begins to damage the alveoli in the infected lungs and releases interferons that signal nearby healthy cells to release antiviral peptides. Antiviral peptides sent to the environment ensure the destruction of viruses. Dead and damaged cells are taken into action to be discarded with the help of cells found in natural immunity. In this case, cytokines are activated, and this chaos in the environment causes the capillaries and alveoli to be filled with liquid. This fluid activates macrophages, which are effective in increasing the infection rate. Neutrophils reaching the infected area attack viruses while damaging the epithelial cells lining the air spaces of the lungs. In this way, decreases in the alveoli surfactant begin (Kumar et al., 2021; Yüce, Filiztekin, and Özkaya, 2021) (*Figure 1-2-1*).

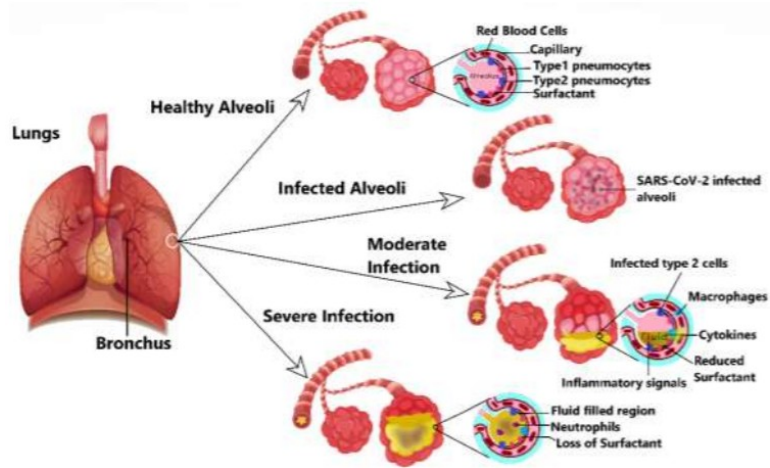


Figure 4-2-1 COVID-19 infection in the lungs at various stages(Kumar et al., 2021).

The phagocytic cells in the environment trigger the inflammatory cells that cause inflammation and cause them to secrete. This immune response is called a cytokine storm. In the case of very severe infection, systemic inflammatory response syndrome (SIRS) may occur when protein-rich fluid enters the bloodstream. In this case, multi-organ failure can be seen. Due to infection, their receptors on the cranial nerve can be activated and produce a cough response in the central nervous system. The hypothalamus may be affected due to the inflammation and the chaos in the lungs, and an increase in body temperature may be observed(Kumar et al., 2021).

1.3 Symptoms of Covid-19

After the virus has completely passed the carrier process, the time reported by the World Health Organization for the virus to show its active effect is 5-6 days. Infected people show different symptoms. Most common: Fever, Dry cough, tiredness. Less common: Body pain, Sore throat, Tiredness and headache, Diarrhea, Skin rashes, Loss of taste or smell. Very severe symptoms: Conjunctivitis, Bluish lips or face, Loss of speech or movement, Inability to stay awake, Shortness of breath (Centers for Disease Control and Prevention, 2021). As for the organs affected by the infection, it affects almost all vital organs. With the effect of acute respiratory distress syndrome, the vessels are affected and when there is excessive ACE2 distribution, the disease-killing effect increases, and

mass organ failure begins. Individuals with circulatory and respiratory disorders and smokers may be more affected by Covid-19(Berlin et al., 2020).

1.4 Diagnosis

A nasal swab, tracheal aspirate, or bronchoalveolar lavage (BAL) material is used in the RT-PCR diagnostic test (Giuseppe Pascarella, 2020). The primary and preferred method for diagnosis is the collection of upper respiratory tract samples via nasal and oral swabs. Samples taken are quickly analyzed using RT-PCR. In addition, it is possible to control Covid-19 with blood samples. The rate of IgM antibodies in the blood gives information after the 7th day of the disease. In addition to these procedures, another known method is Imaging- Chest X-Ray and CT scan. This last method is generally used to see the lung condition of patients with positive PCR tests(Kumar and Lupoli, 2020).

1.5 Treatments

There is no active method for the treatment of SARS-CoV-2 infection yet. Most current treatments. It is intended to relieve symptoms or support immunity. In SARS-CoV-2 disease, viral drugs used previously for treatment in MERS, HIV, SARS, Ebola viruses were tried (Pardo et al., 2020). While patients with severe symptoms are treated with drugs. Patients with milder symptoms: first of all, it is encouraged to be isolated and when symptoms increase, drug treatment is applied(Pilkington, Pepperrell and Hill, 2020).

Hydroxychloroquine and Chloroquine: Chloroquine (CQ) and hydroxychloroquine (HCQ) are examples of aminoquinolines used to treat malaria and autoimmune diseases. These are known as antimalarial drugs that have proven to be antiviral agents. They do so by inhibiting the movement of the SARS-CoV virus by preventing the fusion of the virus with the host cell and by interfering with the ACE-2 receptors. In some studies, it has been observed that they can also stop the SARS-COV-2 virus(Pastick et al., 2020). Since the side effects of the drug have been observed in clinical trials, its use has been limited (US FDA, 2020).

Remdesivir: The US FDA has approved this medicine for the treatment of SARS-CoV-2, and it has previously been used to treat Ebola, SARS-CoV, and MERS-CoV infections (Pardo et al., 2020). Remdesivir blocks the RNA-dependent RNA polymerase enzyme that the virus needs for replication (*Figure 1-5-1*). Based on NIAID trials, reductions in mortality were observed when Remdesivir was used. In addition to the positive effect of the drug, it has been observed that some patients have serious side effects, including liver damage (Yin et al., n.d.).

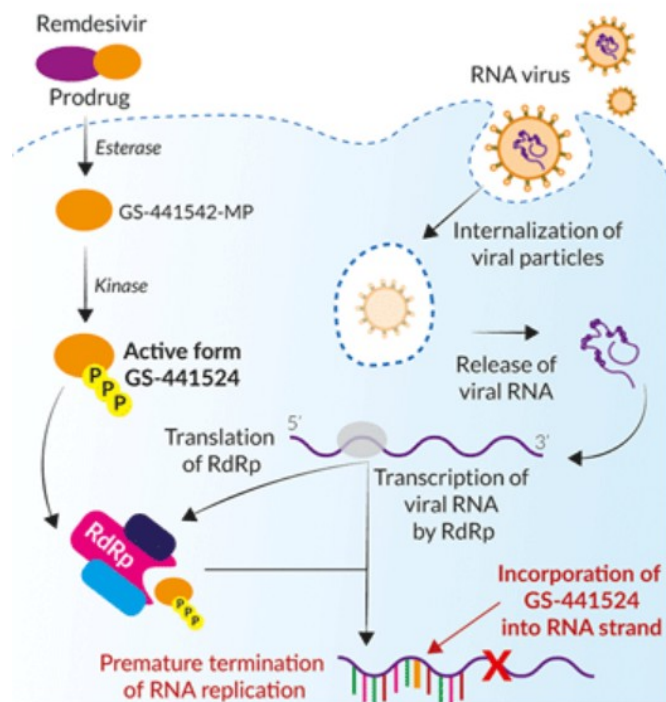


Figure 1-5-5 Remdesivir mode of action. (invivogen.com, n.d.)

Favipiravir: It is a drug approved in Japan since March 2014 for the treatment of severe influenza cases. It is a strong antiviral that inhibits the RNA-dependent RNA polymerase enzyme of RNA viruses. It is also among the drugs tested for SARS-CoV-2. The drug was successfully tested on 70 patients and was approved (COVID-19: Finding the Right Fit Identifying Potential Treatments Using a Data-Driven Approach, n.d.).

In addition to these drug treatments, many drugs are used and tested in the treatment process, there are also plasma therapies and vaccine studies, but this study will not be detailed because it was not very effective on them.

1.6 RNA-dependent RNA polymerases (RdRp)

RdRPs (RNA-dependent RNA polymerases) are viral RNA-dependent RNA polymerases that play a crucial role in viral genome replication and transcription. To accomplish completely RNA-based genome replication and transcription, RNA viruses encode a unique class of RNA-dependent RNA polymerases (RdRps). Although all nucleic acid polymerases share the chemical basis of nucleotide addition, the structural and mechanical characteristics adopted by each polymerase class differ to variable degrees (Shu and Gong, 2016).

1.7 Ligand-Based Drug Design

The structure of the protein or the biological and physicochemical properties of the bound ligands are the two categories of methodologies utilized in computer-aided drug creation. In recent years, structural-based and ligand-based pharmacophore modeling has been used to improve the reliability and efficiency of computer-aided drug design methodologies by incorporating information from both ligand and protein (Wilson and Lill, 2011). In the lack of recipient 3D knowledge, ligand-based drug design is the preferable strategy. The knowledge of chemicals that bind to the biological target of interest underpins this strategy. In ligand-based drug design, 3D quantitative structure-activity correlations and pharmacophore modeling are significant and frequent methods. As a result, relevant prediction models for lead identification and optimization can be built (Aparoy, Reddy, and Reddanna, 2012).

2. MATERIALS AND METHODS

In this research, “7bv2.pdb” and “6m71.pdb” enzymes were used as macromolecule structures. 7bv2.pdb is the structure of The nsp12-nsp7-nsp8 complex bound to the template-primer RNA and triphosphate form of Remdesivir (RTP). 6m71.pdb: SARS-Cov-2 is the structure of RNA-dependent RNA polymerase in complex with cofactors. These pdb constructs were obtained from the RCSB's Protein Data Bank (<https://www.rcsb.org/>).

The above-mentioned enzyme constructs were included in the processes with The SARS-CoV-2 Helicase Targeted Library prepared by the OTAVA chemicals database. To get this library, it is possible to reach OTAVA chemicals via e-mail (mol.design@otavachemicals.com) and share the project information when requested. There are 1176 ligands in the .sdf format library sent by OTAVA chemicals.

2.1 Protein Preparation

The technique of finding the lowest energy conformation of a molecule is known as energy minimization. The low energy structure can be calculated using the lowest steric energy bond lengths and angles. Bonds are rotated in the atomic position within the system and calculates the energy for each position. Geometry cleaning is the process of repeating this operation till the least energy is reached. Each movement must lower the energy; otherwise, the atom will return to its original (initial) position. Minimization refers to the complete rotation of an atom (Karamertzanis and Price, 2006).

The nsp12-nsp7-nsp8 complex is attached to the template-primary RNA and triphosphate form of Remdesivir (RTP), that is, when the 7bv2.pdb file is opened via RCSB, the enzyme has three chains: A (RNA-directed RNA polymerase), B (Non-structural protein

8), C (Non-structural protein 7). In addition to these chains, there are a ligand and three different activators in the macromolecule (**Figure 2-1-1**). These activators are POP (PYROPHOSPHATE 2-), zinc ion, and magnesium ion. As for the ligand: F86 (2~{R},3~{S},4~{R},5~{R})-5-(4-azanylpyrrolo[2,1-f][1,2,4]triazin-7-yl)-5-cyano-3,4-bis(oxidanyl)oxolan-2-yl]methyl dihydrogen phosphate) also known as Remdesivir, bound form. The structure is in the viral protein class and its solubility value is 2.50 Å. The organism of the structure severe acute respiratory syndrome coronavirus 2 and the system in which it is synthesized is Spodoptera frugiperda.



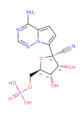


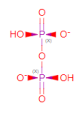




<p>F86 (Subject of Investigation/LOI) Query on F86</p> <p>Download Ideal Coordinates CCD File </p> <p>Download Instance Coordinates </p>	<p>K [auth P] [(2~{R},3~{S},4~{R},5~{R})-5-(4-azanylpyrrolo[2,1-f][1,2,4]triazin-7-yl)-5-cyano-3,4-bis(oxidanyl)oxolan-2-yl]methyl dihydrogen phosphate</p> <p>C₁₂ H₁₄ N₅ O₇ P ZBHOHJWLOOFLMW-LTGWCKQJSA-N</p>	
<p>POP Query on POP</p> <p>Download Ideal Coordinates CCD File </p> <p>Download Instance Coordinates </p>	<p>H [auth A] PYROPHOSPHATE 2-</p> <p>H₂ O₇ P₂ XPPKVPWEQAFLFU-UHFFFAOYSA-L</p>	
<p>ZN Query on ZN</p> <p>Download Ideal Coordinates CCD File </p> <p>Download Instance Coordinates </p>	<p>F [auth A], G [auth A] ZINC ION</p> <p>Zn PTFCDOFLOPIGGS-UHFFFAOYSA-N</p>	<p>Zn⁺²</p>
<p>MG Query on MG</p> <p>Download Ideal Coordinates CCD File </p> <p>Download Instance Coordinates </p>	<p>I [auth A], J [auth A] MAGNESIUM ION</p> <p>Mg JLVVSXFLKOJNIIY-UHFFFAOYSA-N</p>	<p>Mg⁺²</p>

Figure 2-1-6 Ligand and activator information of 7bv2.

BIOVIA Discovery Studio was used to accurately prepare the macromolecule structure. In this operation, the pdb file of the 7bv2 enzyme, which we downloaded from RCSB, was first uploaded to the system. When we load it into the system, we can see the chains, ligand, active sites, ions, and water of the structure in more detail, as in **Figure 2-1-2**. During the visual inspection of the structure, we also observe that it contains a nucleic acid group (purine, pyrimidine, phosphate, sugar, etc.) (**Figure 2-1-2**).

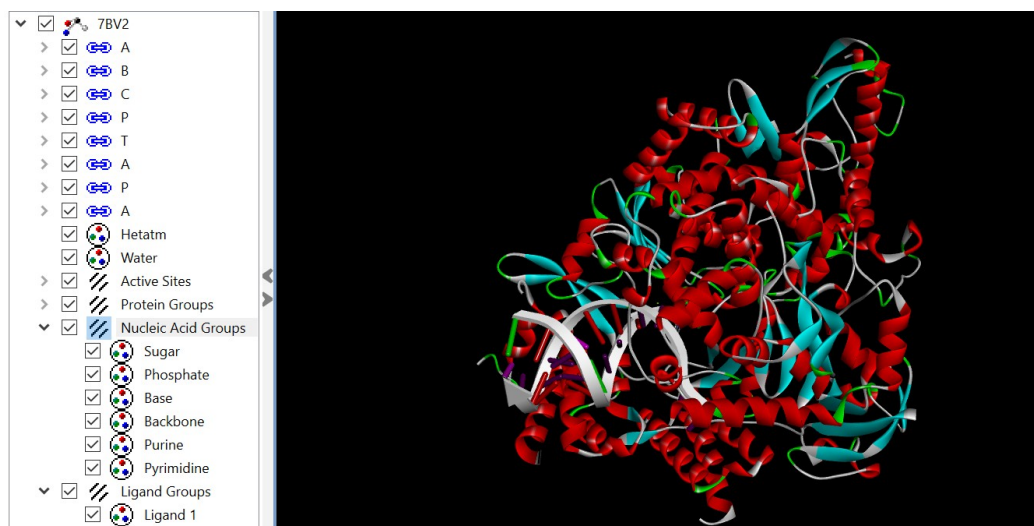


Figure 2-1-7 Discovery Studio information of 7bv2.pdb.

After the structure analysis of 7bv2.pdb was finished, the process of locating the ligand was started. The ligand group was selected in the explanatory panel of the Discovery studio application. The selected ligand was colored yellow and 'From Current Selection' was clicked under the 'define and Edit Binding Site' button. As a result of these processes, a sphere surrounding the ligand was formed. The size of this formed sphere was enlarged to encompass all the edges of the ligand. The resulting sphere is an important guide that will inform us where to place the other ligand during the docking phase. To get the coordinates of the sphere: After clicking on the sphere, using the right click of the mouse, 'Attributes of sphere object' must be clicked and the coordinates of the sphere appear as in **Figure 2-1-3**.

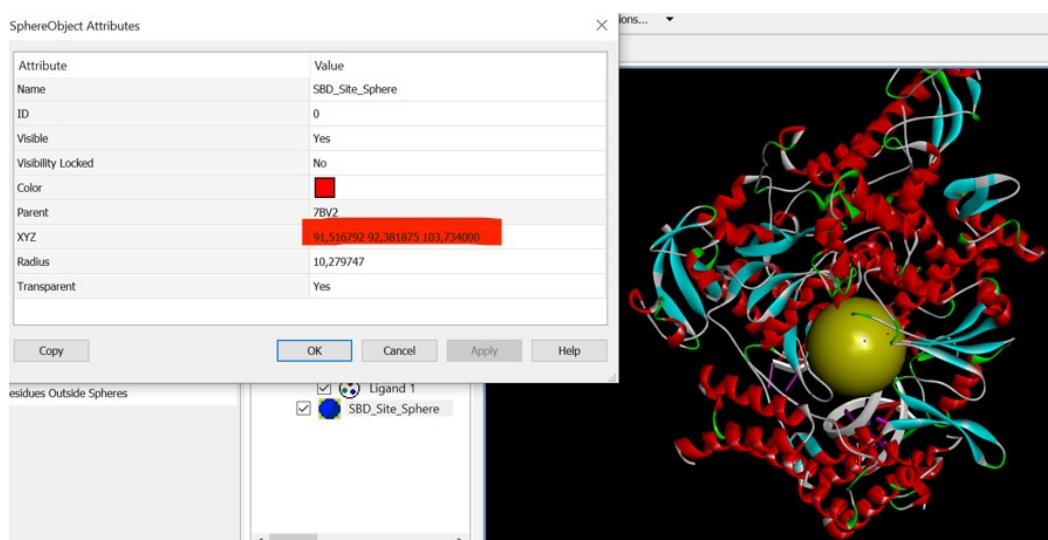


Figure 2-1-8 7bv2's ligand coordinates were found using the sphere.

After this process, all ligand structures, water, etc. found in this macromolecule were deleted as shown in **Figure 2-1-4**. The energy minimization process was done. Pdb structure was created as shown in **Figure 2-1-5**.

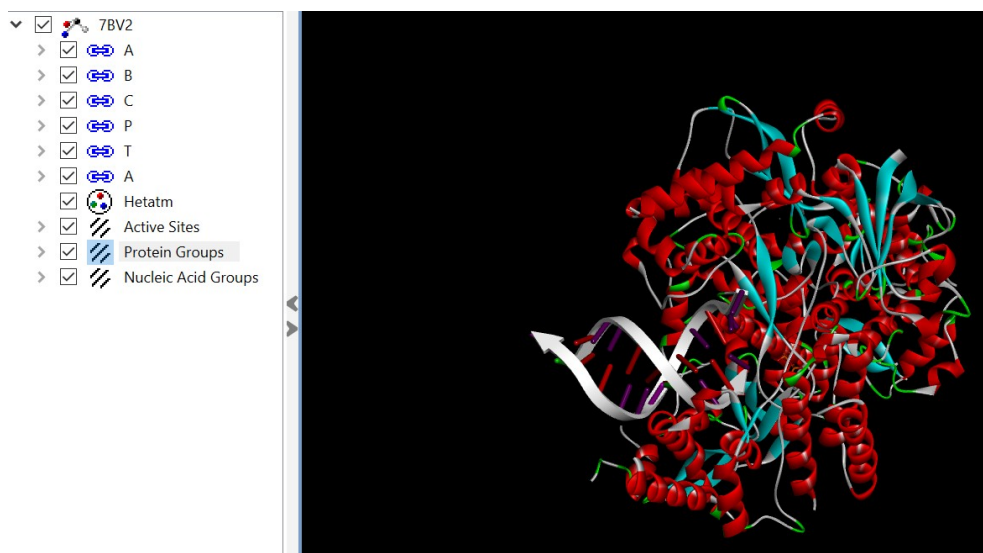


Figure 2-1-9 Preparation of macromolecule 7bv2.

To minimize the energy, the red arrow next to the H sign should be clicked on from the menu that appears when the mouse is right-clicked on the molecule. When this arrow is clicked, clean geometry text will be seen. This process takes some time and causes a change in the shape of the molecule. As seen in **Figure 2-1-5**, the color of some alpha and beta images turns green. Since this structure is more stable, it will enable us to get better results.

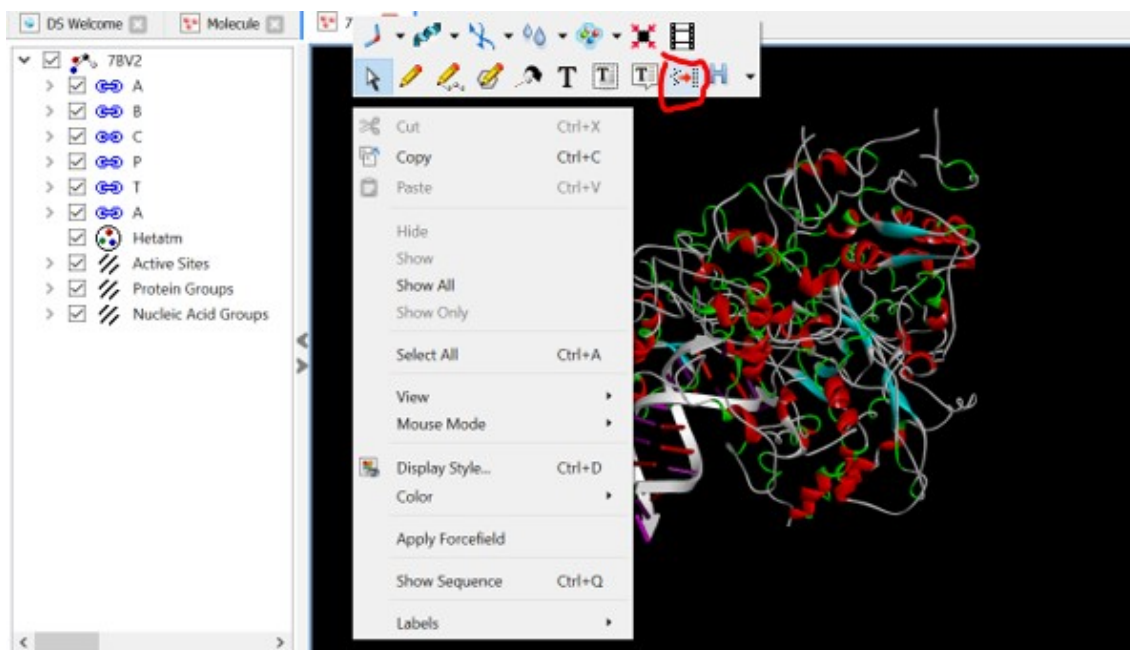


Figure 2-1-10 Energy minimization (clean geometry) process.

The other enzyme structure I chose to use in this study is the molecule 6m71.pdb. The pdb structure was taken from the RCSB protein database, like other molecules, by making evaluations. The considerations were: crystallization (modelling) of the molecule after 2019, low solubility, and selected based on features such as previous use in studies related to Covid-19.

6m71.pdb was downloaded from the RCSB protein database. After general examinations, it was realized that the enzyme did not have a significant ligand, so different studies were needed to find out where the active site of the enzyme was. The publication containing information about the enzyme in RCSB was reviewed, and it was learned that the active site contained A623 residue in the publication (Gao et al., 2020). After downloading the pdb, it was opened with the help of the notebook application, and point A623 was found. The XYZ coordinates of this point were determined as: 120.142 120.563 127.503. In the general analysis of the pdb file, it was determined that the resolution was 2.90 Å.



Figure 2-1-11 Discovery Studio information of 6m71.pdb

When the pdb structure is opened with the help of Discovery studio, we encounter the structure in **Figure 2-1-6**. As I have said before, there is no ligand in the structure, and we have seen this in the figure. When the structure is examined visually, it is observed that it consists of 4 chains, but the structure has 3 unique chains. During the visual inspection of the structure, we also observe that it contains protein groups (disulfide, sidechain, backbone, neutral, acidic, basic, etc.) (**Figure2-1-7**).



Figure 2-1-12 Protein groups information of 6m71.pdb

The red arrow adjacent to the H sign should be clicked on from the option that comes when the mouse is right-clicked on the molecule to lower the energy. When you click this arrow, you'll see clean geometry lettering. This procedure takes some time and results in a change in the molecule's shape. The color of some alpha and beta images turns green, as shown in *Figure 2-1-8*. We will be able to achieve better results because this structure is more stable.

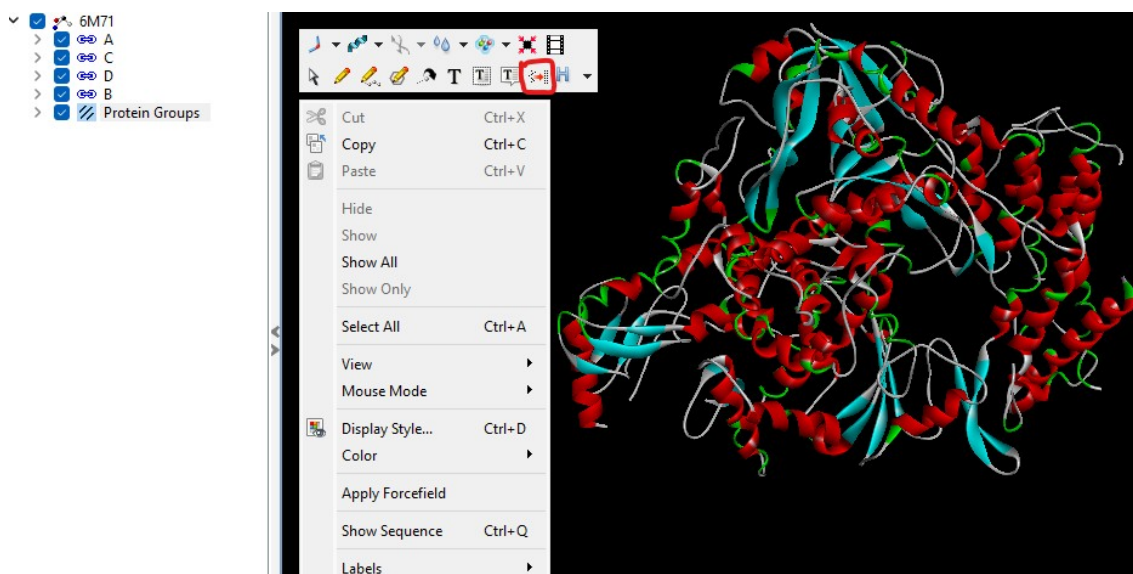


Figure 2-1-13 Energy minimization (clean geometry) process.

After the structural evaluation and preparation of both models, they were both saved in .pdb format. This procedure is necessary for the preparation of the docking phase.

2.2 Ligand Preparation

The ligands to be used in this study were requested from the virus database in OTAVA chemicals: SARS-CoV-2 Helicase Targeted Library. For coronaviral replication, the SARS-CoV-2 helicase (non-structural protein 13, NSP13) is required. It distinguishes between double-stranded and single-stranded RNA (dsRNA). The discovery of small compounds that directly target the replication apparatus has shown the greatest promise for antiviral medication development.

OTAVA has a SARS-CoV-2 Helicase (NSP13) Targeted Library with 1170 chemicals that have been shown to have efficacy against this important protein. The library was

created utilizing a receptor-based virtual screening method and a SARS-CoV-2 NSP13 homology model. Drug-like Green Collection was docked onto the active site of the helicase in a precise and flexible manner. The final compound selection was based on an examination of the important structural factors for ligand binding in the enzyme active site, docking scores, and intermolecular hydrogen bonds with key active site amino acid residues (OTAVA chemicals, n.d.).

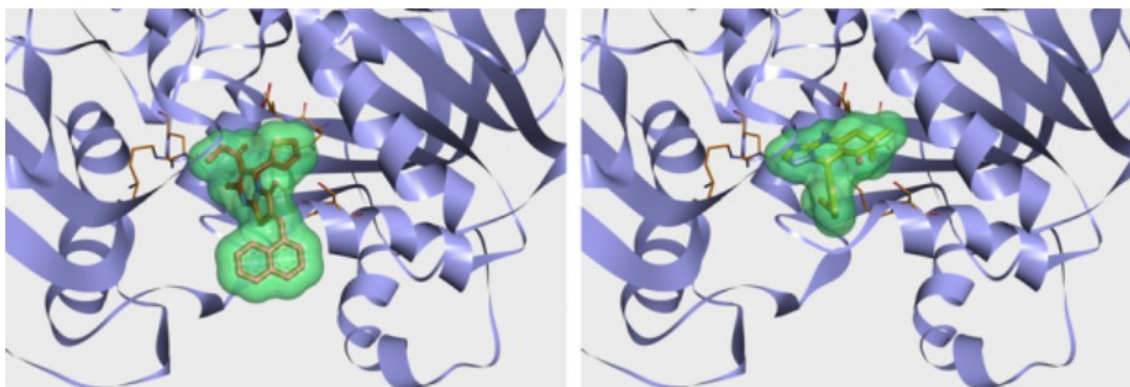


Figure 2-2-1 Example of ligand compounds with NSP13 produced using molecular docking. (OTAVA chemicals, n.d.)

To share this data, the address "mol.design@otavachemicals.com" has been reached. I gave information about the project planned to be done via e-mail and information was shared with me in this way. After the e-mail was sent, a sharing was made in the form of the ligands to be used in this study that was requested from the virus database in OTAVA chemicals('OTAVA_SARS-CoV-2_RNA-dependent_RNA-Polymerase(RdRp)-Targeted-Library.sdf.zip'). When the file in .sdf format was opened, it was observed that there were 1170 ligands in it. The preparation procedure for the use of these ligands was initiated. First, the .sdf file was opened using Dsv (Discovery Studio). Polar hydrogen was added to the ligands one by one, and then clean geometry was performed to ensure stability. At the end of these procedures, ligands were re-registered in .sdf format. Due to the conformations of some ligands, the structure we loaded as 1170 ligands increased to 1336 in the prepared file.

2.3 Docking Process

The goal of molecular docking is to use mathematical methods to approximate the structure of the ligand-receptor complex. The contributions of the hydrogen bond, ionic,

hydrophobic, and van der Waals interactions between the protein and ligand were used to compute it. It's used as a filter to locate the best optimal conformation and interactions of each hit molecule at the protein's active site. The insertion can be done in two processes, each of which is handled independently: first, the ligand conformations in the active area of the protein are demonstrated, and then these adaptations are assessed. The sampling methods should, in theory, be able to duplicate the experimental binding mode, and all forms generated by the scoring function should be at the top of the list (must have the best transmission energy). With these two steps, you'll get a quick review of basic placement theory (Meng et al., n.d.).

PyRx is virtual screening software for computer-aided drug discovery. PyRx was used as a multi and fast docking program for this research to reduce the result amount of similar structures.

The otava_prep.sdf file prepared using PyRx was opened using openBabel in PyRx. In the opened file, all ligands were selected and the selected structures were minimized. This process was completed in a few minutes, and then all the structures were selected again and converted to .pdbqt format. The names of the ligands were formed from compound1 to compound1337. Generated ligands have been added to the 'Vina Wizard' section in PyRx. Afterward, the macromolecule button was clicked to dock the ligands and the 7bv2 and 6m71 pdbs we prepared in Dsv were also uploaded to the system. First, the 7bv2 macromolecule was treated with all ligands. The processing time took about 22 hours and the results were exported as an excel file. The same process was performed for the other macromolecule, 6m71, and it has waited during the first process and the results obtained from it were exported as excel.

The first 20 compounds with the highest binding energy of the table taken out in excel are shared in **Table 3-1-1**. Compounds with the best 5 values were selected from **Table 3-1-1** and they were started to be prepared for Autodock docking. The first 20 compounds with the highest binding energy of the table taken out in excel are shared in **Table 3-1-2**. Compounds with the best 5 values were selected from **Table 3-1-2** and they were started to be prepared for Autodock docking.

Firstly, the MGLTools application was downloaded from '<https://ccsb.scripps.edu/mgltools/downloads/>'. After the download of the application was completed, operations started on the AutodockTools symbol. First of all, the inside

of the file to work with is set in the preferences section. First, the ligand structure was selected as shown in *Figure 2-3-1*. The process was first started with the ligand molecule1143, which is completely optional. After the ligand was selected, the information of the bonds was obtained and the system was approved. after these processes, it was recorded as ligand molecule1 143.pdbqt (*Figure 2-3-2*).

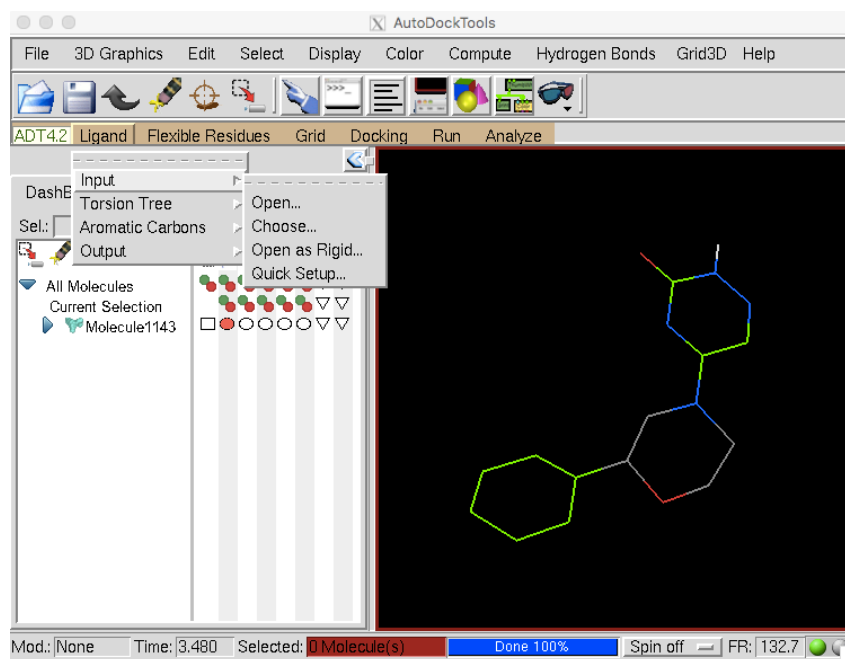


Figure 2-3-1 The start of docking preparations in Autodock Tools.

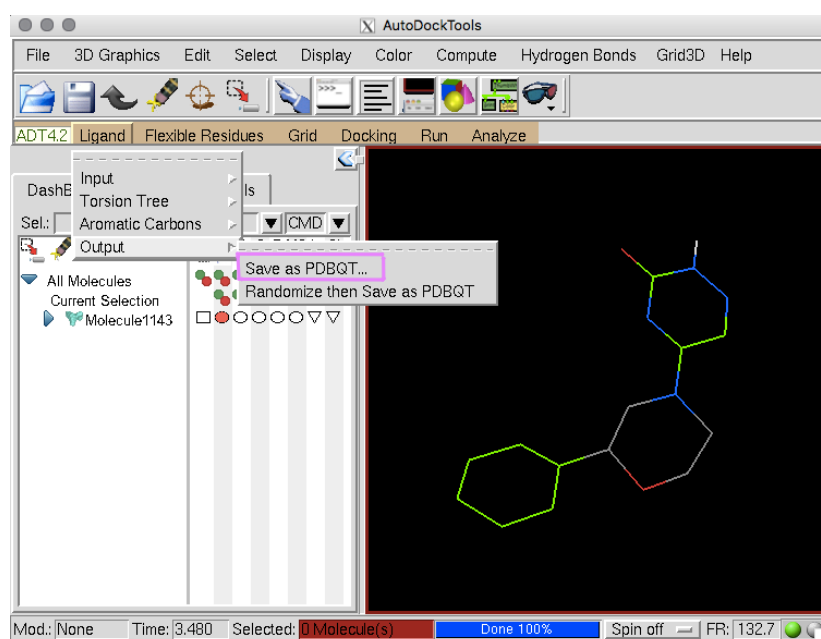


Figure 2-3-2 Saving the ligand in .pdbqt format.

In the next step, the macromolecule 6m71.pdb was loaded into the system as shown in **Figure 2-3-3**. Then the ligand loaded from the "Set Map Types" section was selected. All of these steps are necessary and important steps to create a grid parameter file. **Figure 2-3-5** shows the state of the enzyme after loading. ligand and macromolecule stand independently of each other. The purpose of docking is that these two shapes create a compact structure.

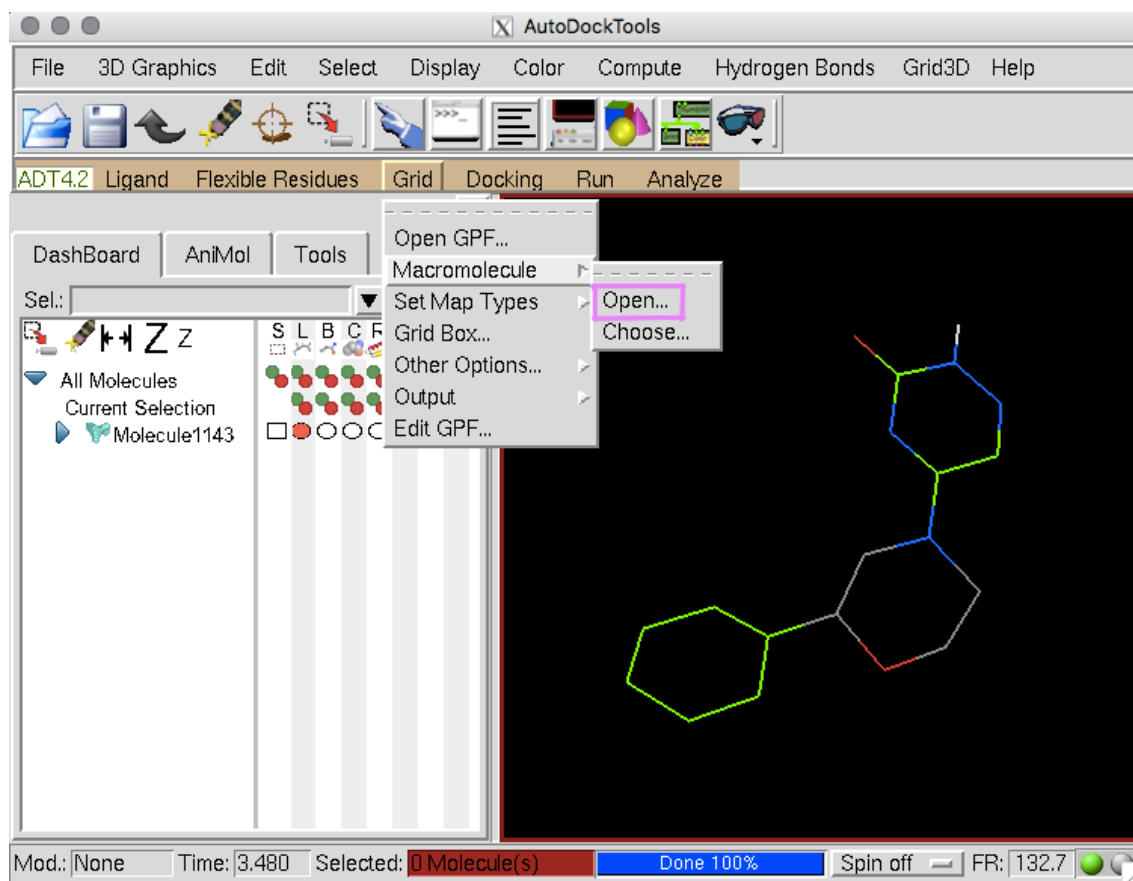


Figure 2-3-4 Uploading macromolecules to Autodock tools.

The last step to create the grid file is the "Grid Box" option. When we click on this option, the opened parameters are updated as in **Figure 2-3-4**. If we come to the meanings of these parameters: 60 60 60 grid was used, 120.142 120.563 127.503 XYZ coordinates that we found in Dsv studio were used as the central measure of the grid. Finally, the file is saved as molecule1143.gpf. The purpose of this process is to give information on which coordinates this new ligand will be placed on the active site of the macromolecule we have.

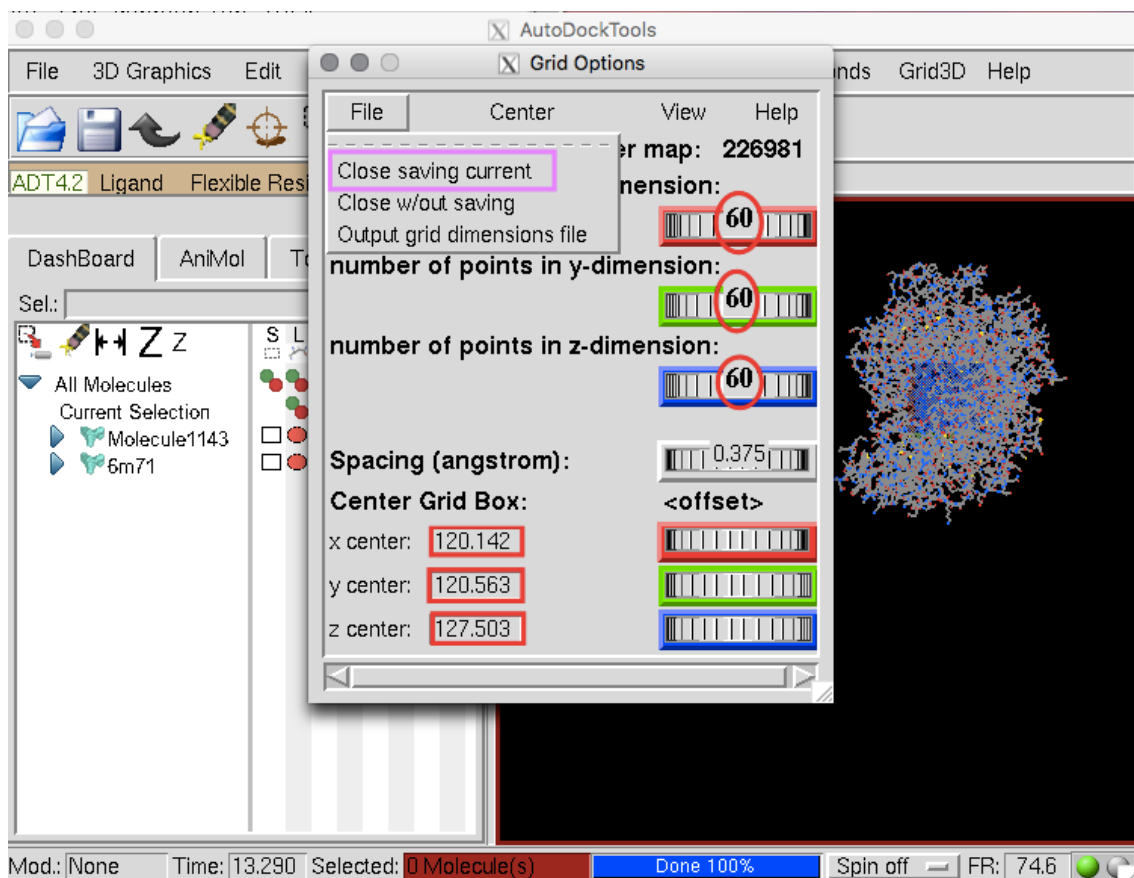


Figure 2-3-5 Grid parameters of 6m71 enzyme.

In addition to the auto grid, After these processes, the docking parameter file preparation process was started. In this process, first macromolecule and ligand are introduced back into the system and then the Lamarckian genetic algorithm is used in autodock4 to obtain optimal insertion conformations. As seen in **Figure 2-3-5**, the Maximum Number of evals options is set to 25.000.000 (long). Finally, the molecule1143.dpf file is saved as output.

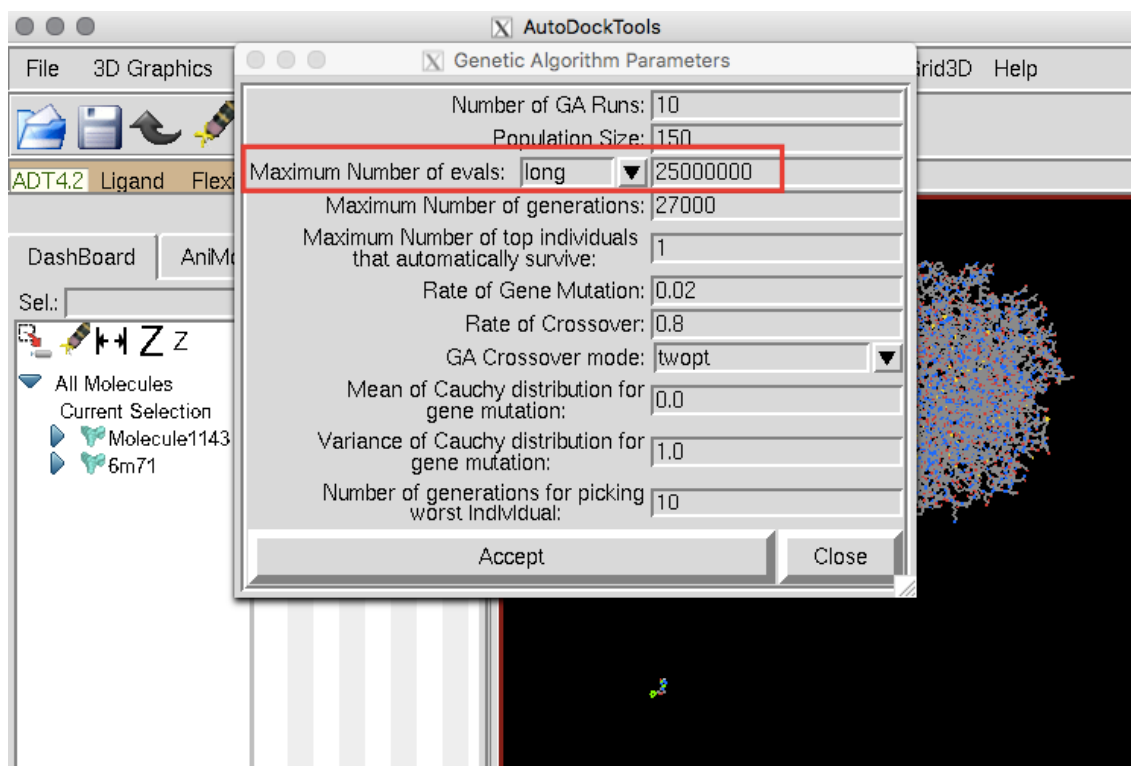


Figure 2-3-6 Lamarckian Genetic algorithm values.

The best binding energies obtained for the two enzymes are shown in **Table 3-1-1** and **Table 3-1-2** in the results section. All processes applied to 6m71.pdb and molecule1143 with the detailed explanation above were applied to 10 molecules shown in the tables to create ‘.gpf’ and ‘.dpf’. As a result of the operations performed on Autodock Tools, .pdbqt files of 2 macromolecules and .dpf and gpf files of 10 ligands were created.

Prepared parameter files need a final process to convert to log files. This process is the docking stage on the Linux Terminal. Although we get faster results in the vina process, Autodock4 gives clearer answers when it comes to binding energies (Trott and Olson, 2009). For this reason, .gpf files should be converted to .glg via terminal first and .dpf files should be converted to .dlg with the parameters taken from them. If we give an example of these codes from the files I prepared:

```
% autogrid4 -p molecule1143.gpf -l molecule1143.glg ; autodock4 -p molecule1143.dpf -l molecule1143.dlg (Morris et al., 1991)
```

The processes continued to be completed so that there are 10 dlg files in total. Among these dlg files, the two ligands with the highest binding energy for both enzymes were selected and 2D and 3D interaction images were extracted.

2.4 ADMET Property Prediction

The abbreviation ADME stands for pharmacokinetics, which is a four-letter subject. A stands for absorption, D for distribution, M for metabolism, and E for excretion. The letter T also contains the letter T. Toxicity is represented by the letter T. When these letters and titles are studied one by one, absorption is the phrase used to describe how a drug moves through the bloodstream (Di, 2015). Many oral drugs, for example, are absorbed in the intestines. When a drug enters the body, it travels through the bloodstream until it reaches the domain. The process by which the body transforms a medicine from its original form to an active or inactive metabolite is known as metabolism. Excretion refers to the process of removing substances and their metabolites from the body. Urine or feces are the most common methods of excretion. ADME investigation helps to check for low blood-brain barrier (BBB), optimal solubility, good absorption, non-inhibition to CYP2D6, and non-hepatotoxicity.

Lipinski's rule of five can also be used as a filter to evaluate a compound's absorption and intestinal permeability. Researchers use Lipinski's rule of five to discriminate between drug-like and non-drug compounds. Molecules that fit two or more of these rules can be classified as drugs, and drug similarity can assist forecast the chance of high success or failure (Pardridge, n.d.). Lipinski's first rule is that for optimal absorption, a molecule should have a molecular mass of fewer than 500 Daltons. The second rule is high lipophilicity; for good absorption, LogP must be less than 5. The third rule states that molecules must have less than five hydrogen bond donors. Fourth, molecules must have less than ten hydrogen bond acceptors. There are no rankings for these rules. If two of the rules are met, the molecule is classified as a drug-like molecule (Lipinski, 2004).

Discovery Studio Visualizer ADME Tools: The ADME plugin of the Dsv application was used in the ADME process. First of all, 10 ligands with the highest binding energy in both enzymes were opened with the help of Dsv and all ligands were collected as a single .sdf. In the ADME plugin, ligands were turned on and ADME properties were shaped according to Lipinski's rule of five. As a result, a graph was created. You can see the graph in *Figure 2-4-1*. In addition to these, statistical data are used to better identify accuracy. For example, BBB-95 means that this circle includes chemicals that have a 5%

error. BBB-99 includes chemicals that only show a 1% error percentage. The drugs to be produced can be evaluated according to these two main characteristics.

SwissADME Tools: Each ligand was imported to the SwissADME one by one. Then, the run button was clicked (**Figure 2-4-2**). Physicochemical properties, lipophilicity, water-solubility, pharmacokinetics, and drug-likeness properties were obtained with the SwissADME website. Each of them was downloaded in CSV format. Then, they were assembled in **Table 3-3-1**.

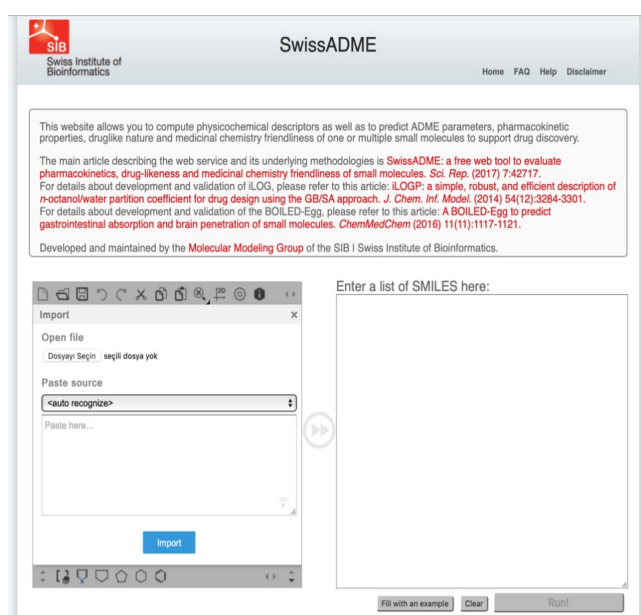


Figure 2-4-2 The SwissADME page. First press the import button then clicks the run button.

Following the completion of all calculations, the red "Show BOILED-Egg" button appears below the sketcher, displaying the graphical outcome on the same page. The BOILED-Egg, for example, is a simple way for predicting two essential ADME characteristics at the same time: passive gastrointestinal absorption (HIA) and brain access (BBB). Although this classification model is conceptually basic, as it only uses two physicochemical markers (LOGP and TPSA, for lipophilicity and apparent polarity, respectively), it was designed with great care in terms of statistical significance and robustness (Daina, Michielin and Zoete, 2017).

The yolk (the dissolution-related area in the blood-brain barrier) and the white (as illustrated in **Figure 2-4-3**) make up the egg-shaped classification plot (the

physicochemical field for highly probable Human intestinal absorption). Both sections are not mutually restrictive, and the outer grey zone represents chemicals with characteristics that suggest low absorption and brain penetration. The BOILED-Egg is simple to read and translate to molecular design in a range of drug discovery scenarios. The BOILED-predictive Egg's potential is vast in chemical space, but it is limited to passive penetration through the gastrointestinal wall and BBB(Daina, Michielin, and Zoete, 2017). Finally, let's talk about PGP⁺ and PGP⁻: PGP⁺ is used for absorbed molecules and the little blue circles represent it in the Boiled-egg diagram. Talking about PGP⁻, it is used for non-absorbed molecules and is indicated by small red circles in the diagram. At the same time, the table on the right side of the diagram shows the molecules that cannot be absorbed (*Figure 2-4-3*).

2.5 Preparation of 2D and 3D interaction maps of Ligands with Macromolecule

BIOVIA Discovery Studio Visualizer (Dsv) was used to view and compare the 2D interactions of ligands with their macromolecules. In this experiment, 1078(7bv2) and 618(6m71) are natural ligands. These two ligands are the ligands with the best binding energy of the enzymes in the docking stage. The process started with finding the best exposure in the .dlg files. the ligand coordinates of the best exposure were opiated and added to the end of the .pdp file of the prepared protein file. The .pdb file in which the two coordinates were combined was opened with Dsv and the 'ligand interaction' button was pressed, and the interactions of the ligand with the macromolecule were revealed. This image was created in 3D. You can see the two interaction diagrams created in *Figure 3-4-2* and *Figure 3-4-3*. After these processes, the 'show 2D diagram' button was pressed to make the bonds made clearer and the bonds made by the ligand to the protein were formed more clearly with their names. you can see this relative in *Figure 3-4-2* and *Figure 3-4-3*.

2.6 Molecular Dynamics Simulation Application using NAMD

Only the best of the almost 2700 chemicals examined was chosen for MD Simulation. In this investigation, the NAMD (<http://www.ks.uiuc.edu/Research/namd/>) simulation tool was used to simulate one molecule (Phillips et al., 2005). The input parameter files for the NAMD MD simulation software are obtained through the CHARMM-GUI web service (<http://www.Charmm.org>) (Kim et al., 2017). The TIP3P water model was used to interpret the system in this online service; water molecules were preserved and neutralized by adding 0.15 M NaCl to the ionic concentration. It was completed during the initial minimization (1000 steps). The system was restarted at 303.15 K using Langevin dynamics after the initial minimization. With a time step of 2 fs for 1 ns, the system reached equilibrium. The system, which prevents water molecules from accessing the membrane's hydrophobic area, is stabilized for 1 ns. Harmonic constraints are removed in the final minimization, further balancing the system. For 50 ns at 303.15 K and 1 atm, the production run was done without any constraints (Phillips et al., 2005). The entries of the process were created as .inp files and the equilibration process was done first. this process took about 5 hours and then. The process has been started to convert the production. inp file to the .log file. Although the process was 50 ns, it took about 90 hours. When the .log file is created, we will be able to calculate the root mean square deviation (RMSD): the fitting is usually done about the beginning structure. The RMSD calculation and fitting do not have to be done using the same set of atoms; for example, a protein is commonly fitted on the backbone atoms, but the RMSD can be estimated for the backbone or the entire protein. The radius of rotation. (R_g), the root means square fluctuation (RMSF) and the energies of the systems. RMSF: The distinction between RMSD and RMSF is that the latter is averaged over time and gives a value for each particle I whereas the RMSD is averaged over all particles and gives time-specific values. R_g : The compactness of a structure is measured in R_g . In the results section, necessary information about the graphics and results will be given.

3. RESULTS

3.1 PyRx Autodock-Vina Results

In this study, The SARS-CoV-2 Helicase Targeted Library (1170 molecule) from OTAVA chemical and two enzymes (6m71, 7bv2) were used. In total, approximately 1336 ligands were obtained through the OTAVACHemicals library. All ligands were processed in the AutoDock-Vina program of the PyRx application using one enzyme together, without discrimination. Except for molecule1 and molecule2 ligand, other 1334 ligands gave more negative values than -5.00 for the 6m71 enzyme. When we look at 7bv2, this number is over 100. After exporting the AutoDock-Vina results of PyRx to excel, the best 20 ligands according to the binding energy are shown in Table 3.1. The fact that a ligand has a positive or near-positive binding energy means that it will be unsuitable for the selected enzymes. After the results were obtained, the best inhibitors of the 7bv2 and 6m71 3enzymes were determined according to the total binding energy score. After selections, the next step Autodock 4 will be started. At this stage, it was decided to make the best five of the ligands screened. the binding energy range in this selection is between -9 and -8.2. We have a total of 10 compounds as we have chosen for two enzymes and both are displayed in separate tables (*Table 3-1-1*)(*Table 3-1-2*).

Table3-1-1 Top 20 binding affinity energies of 6m71.pdb enzyme docked using PyRx-Autodock-Vina.

Ligand	Binding		
	Affinity	rmsd/ub	rmsd/lb
6m71_Compound373	-9.0	0.0	0.0
6m71_Compound966	-9.0	0.0	0.0
6m71_Compound1143	-8.8	0.0	0.0
6m71_Compound321	-8.8	0.0	0.0
6m71_Compound618	-8.8	0.0	0.0
6m71_Compound984	-8.8	0.0	0.0
6m71_Compound1117	-8.7	0.0	0.0
6m71_Compound320	-8.7	0.0	0.0
6m71_Compound72	-8.7	0.0	0.0
6m71_Compound859	-8.7	0.0	0.0
6m71_Compound918	-8.7	0.0	0.0

6m71_Compound1134	-8.6	0.0	0.0
6m71_Compound119	-8.6	0.0	0.0
6m71_Compound1201	-8.6	0.0	0.0
6m71_Compound13	-8.6	0.0	0.0
6m71_Compound153	-8.6	0.0	0.0
6m71_Compound289	-8.6	0.0	0.0
6m71_Compound334	-8.6	0.0	0.0
6m71_Compound410	-8.6	0.0	0.0
6m71_Compound520	-8.6	0.0	0.0

Table 3-1-2 Top 20 binding affinity energies of 7bv2.pdb enzyme docked using PyRx-Autodock-Vina.

Ligand	Binding Affinity	rmsd/ub	rmsd/lb
7bv2_prep_Compound798	-8.5	0.0	0.0
7bv2_prep_Compound817	-8.4	0.0	0.0
7bv2_prep_Compound1078	-8.3	0.0	0.0
7bv2_prep_Compound302	-8.3	0.0	0.0
7bv2_prep_Compound292	-8.2	0.0	0.0
7bv2_prep_Compound78	-8.2	0.0	0.0
7bv2_prep_Compound87	-8.2	0.0	0.0
7bv2_prep_Compound943	-8.2	0.0	0.0
7bv2_prep_Compound1277	-8.1	0.0	0.0
7bv2_prep_Compound303	-8.1	0.0	0.0
7bv2_prep_Compound431	-8.1	0.0	0.0
7bv2_prep_Compound432	-8.1	0.0	0.0
7bv2_prep_Compound83	-8.1	0.0	0.0
7bv2_prep_Compound1071	-8.0	0.0	0.0
7bv2_prep_Compound1225	-8.0	0.0	0.0
7bv2_prep_Compound253	-8.0	0.0	0.0
7bv2_prep_Compound301	-8.0	0.0	0.0
7bv2_prep_Compound431	-8.0	0.0	0.0
7bv2_prep_Compound87	-8.0	0.0	0.0
7bv2_prep_Compound96	-8.0	0.0	0.0

3.2 Autodock4 Results

Table 3-2-1 Binding energy values of the best 5 compounds according to Autodock4 for 6m71.

Ligand	Binding Affinity	Cluster RMSD	Reference RMSD
Molecule321	-7,77	0.00	208.63
Molecule373	-7,54	0.00	209.76
Molecule618	-8,13	0.00	211.04
Molecule966	-5,93	0.00	207.22
Molecule1143	-5,71	0.00	213.14

Computational binding energies of compounds docking with 6m71 enzyme in our RdRp RNA dependent RNA polymerase enzyme (RdRp) are shown in **Table 3-2-1**. Our ligand with the best experimental inhibition value is Molecule618. The 5 compounds used in the AutoDock4 study are ranked from best to worst: Molecule618 > Molecule 321 > Molecule373 > Molecule966 > Molecule1143. The values of the compounds of the other enzyme used are shown in **Table 3-2-2**. After autodock, this enzyme gives the best value. The most successful compound of the enzyme is the ligand Molecule1078. The binding affinity value is the highest and most successful among the dockings made with -8.77. If the other compounds are sequenced from largest to smallest for the 7bv2 enzyme, the sequence Molecule1078 > Molecule817 > Molecule798 > Molecule302 > Molecule292 is obtained.

Table 3-2-2 Binding energy values of the best 5 compounds according to Autodock4 for 7bv2.

Ligand	Binding Affinity	Cluster RMSD	Reference RMSD
Molecule292	-6.73	0.00	164.54
Molecule302	-7.00	0.00	167.38
Molecule798	-7.43	0.00	157.62
Molecule817	-8.11	0.00	167.40
Molecule1078	-8.77	0.00	159.41

3.3 ADMET Application Results

In this step, the predicted drug-like and ADMET properties of 10 potent inhibitors of 6m71, 7bv2 enzymes were investigated. Composite codes determined after docking steps among all ligands in .sdf format were converted into a single .sdf file. The construct that opened only 10 ligands created was opened using the ADME tool of Biovia Discovery Studio Visualization (Dassault Systems BIOVIA, 2021).

ADME features: Lipinski "rule of five", Veber's Rule, Molecular Weight (MW) (gr/mol), MLogP, Aqueous Solubility (Aq. Sol. LogS), Number of Rotatable Bonds, Hydrogen Bond Acceptor (HBA), Hydrogen Bond Donor (HBD), Topological polar surface area (TPSA (\AA^2)) is given as shown in **Table 3-3-1**.

Table 3-3-1 SwissAdme ADME properties.

Compound Name	Lipinski Rule	Veber's Rule	Molecular Weight (gr/mol)	MlogP	Aq. Sol. (LogS)	Number		TPSA (\AA^2)	
						of Rotatable Bonds	Hydrogen Bond Acceptor		
Molecule292	Yes	Yes	491.77	3.9	-8.60	5	6	2	123.32
Molecule302	Yes	Yes	489.53	4.2	-6.30	4	4	1	77.62
Molecule321	Yes	Yes	494.75	4.2	-5.00	5	7	1	102.01
Molecule373	Yes	Yes	418.63	4.2	-4.30	2	6	0	88.59
Molecule618	Yes	Yes	410.65	4.2	-3.30	1	6	0	57.23
Molecule798	Yes	Yes	467.77	4.4	-7.10	5	6	1	134.72
Molecule817	Yes	Yes	404.65	2.8	-3.80	3	4	0	85.19
Molecule966	Yes	Yes	507.91	4.1	-6.40	2	6	1	85.19
Molecule1078	Yes	Yes	382.62	3.7	-5.40	3	4	1	85.19
Molecule1143	Yes	Yes	277.43	2.7	-4.90	2	4	1	85.19

MlogP: (Moriguchi model of octanol-water partition coefficient, LogP) ≤ 5 . **LogS:** Aqueous Solubility > -5.7 **Mw:** Molecular weight in ≤ 500 Da. **HBA:** Total number of H-bond acceptors, N and O ≤ 10 . **HBD:** Total number of H-bond donors, NH and OH ≤ 5 . **TPSA:** Topological polar surface area $\leq 140 \text{\AA}^2$.

The number of hydrogen bond donors varies between 0 and 2, and the number of hydrogen bond acceptors varies between 4 and 7. According to Lipinski's rule of five, hydrogen bond donors must be less than 5 and hydrogen bond acceptors less than 10. With this in mind, it can be said that the compounds comply with the first two rules.

LogP is another important value indicating lipophilicity and according to Lipinski's rule of five, the logP value should be ≤ 5 . The LogP value was below 5 for all compounds used in this study. LogS is the aqueous solubility estimated from the molecular structure and while other molecules except Molecule292 dissolve more easily, Molecule292 can be said to be slightly more resistant with a value of -8.60 (*Table 3-3-1*).

Lipinski's law was taken into account when evaluating in terms of molecular weight. this rule requires a molecular mass of ≤ 500 . All but one of the 10 structures scanned fully meet this rule. Molekul966 slightly exceeded the limit with 507.91 (*Table 3-3-1*). However, the system did not see a problem in violation of a rule and evaluated the molecule positively.

The total polar surface area (TPSA) of a molecule is critical for its transit through biological membranes. A drug's bioavailability and absorption are hampered by high TPSA values. The absorption percentages calculated for the 10 molecules examined ranged from 57% to 135%. Any molecule that breaks more than one of these criteria is likely to have low oral bioavailability and absorption (Lipinski, 2004).

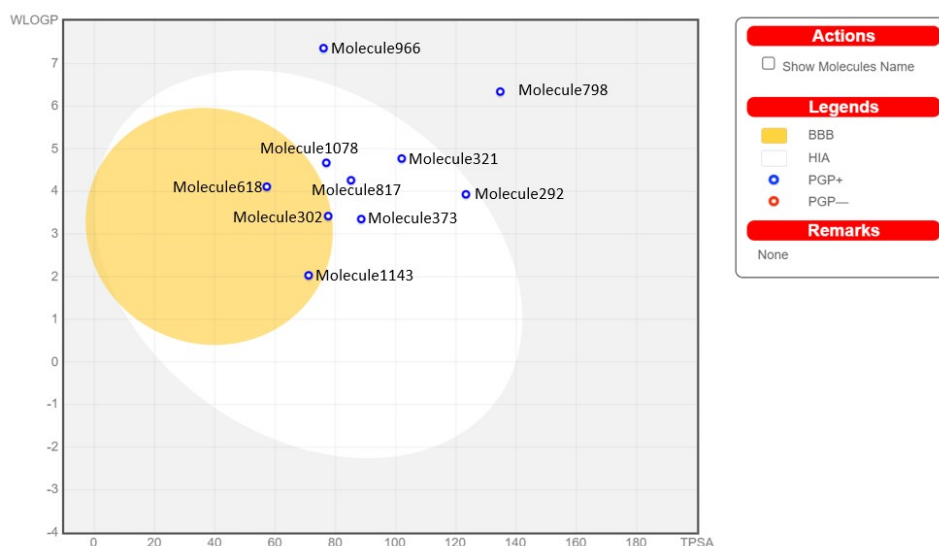


Figure 2-4-3 BOILED-predictive Egg's model for the top 10 drug precursor compounds.

Figure 2-4-3 shows the Boiled Egg prediction model. There are three different ellipses in the model. The yolk BBB point is the absorption point. The white part, which is

exhibited as the white of the egg, gives information about gastrointestinal absorption. If we talk about the gray ellipse, that area is the area where absorption is minimal (Shweta, Rashmi, and Mishra, 2011). In this study, ten molecules were screened. When the points are counted, it is seen that all the selected molecules provide absorption and somehow comply with this rule. It is observed that other structures, except Molecule966 and Molecule798, are more successful in dissolving. While Molecule618 and Molecule302 are successfully absorbed in the BBB point; The other six molecular structures ensured successful absorption in the gastrointestinal tract.

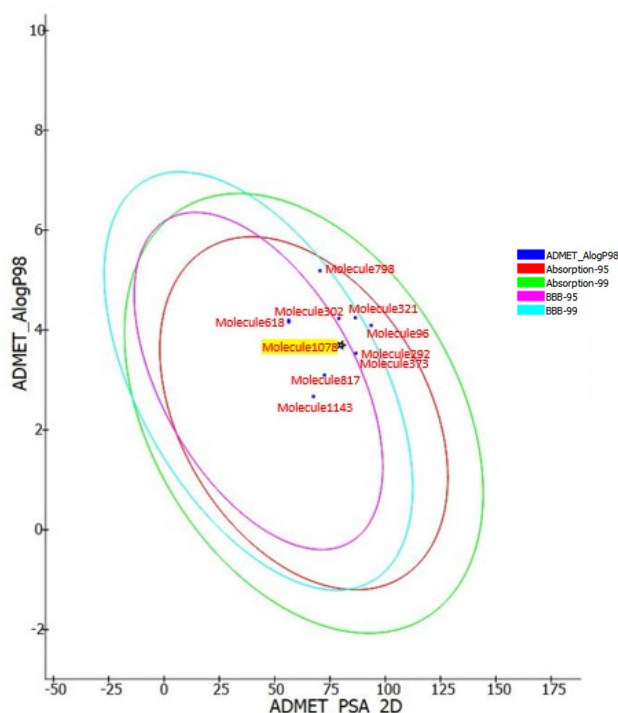


Figure 2-4-1 Discovery Studio Visualizer ADMET tool graphical result.

In this study, a separate ADME study was conducted in Discovery Studio as well as SwissADME. For this process, the best 10 ligands were selected according to their post-docking binding energies. ADME was made for each of these ligands and no structure was observed that did not comply with ADME conditions as well as absorption. Some of the ligands were absorbable abdominally, while others were also absorbed in the BBB. ligands in the purple and light blue rings can pass through the BBB; green and red rings are effective on abdominal absorption. In this study, in which we created two different

graphs, **Figure 2-4-1** and **Figure 2-4-3** graphs give different results when compared. For example, the Molecule1078 structure gives the best docking value; While this structure is resolved in 95% BBB in the Dsv tool, it is said that it is resolved in the abdominal area in SwissADME. This may be due to the parameters that the applications use internally. In general, Dsv gives more detailed information when examined and compared. For this reason, it may be possible to observe changes between structures.

3.4 2D and 3D Diagram Results

2D and 3D images of the interaction of reference compound 7bv2 with its ligand (F86) are given in **Figure 3-4-1** for comparison with other ligands.

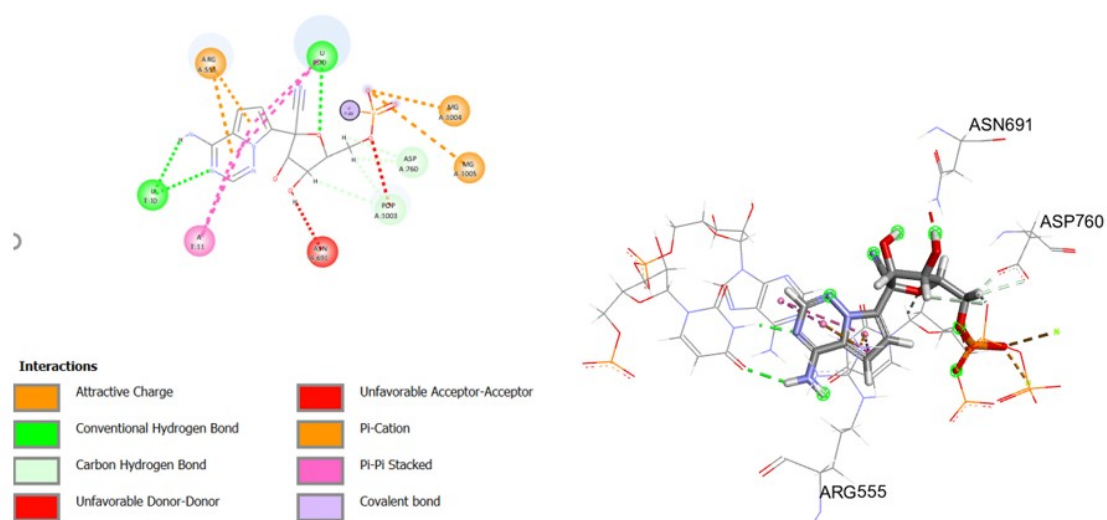


Figure 3-4-1 2D and 3D images of compound 7bv2 and its original ligand (F86).

2D and 3D images of the interaction of reference compound 7bv2 with its ligand (F86) are given in Figure 3.1 for comparison with other ligands. Among the shapes created, it is observed that the 2D diagram is more informative and explanatory than the 3D diagram. In the first evaluation of the RdRp enzyme, its ligand in crystallized form was used. It is seen that the structure, which structurally contains a ligand (F86) and 3 cofactors (POP, Mg, Zn), makes eight different interactions. It makes the Attractive charge interaction, which is shown in orange, which the ARG555 does. to define it: Coulomb force is the

force that exists between two or more charged things as a result of Coulomb's law. The force is repulsive if the particles are both positively and negatively charged, and attractive if they are oppositely charged (Popa et al., 2010). The second interaction is Conventional Hydrogen Bond. It was made at two different points. This means that hydrogen bonds to an electronegative atom at two points and are partially charged with a positive charge, resulting in a strong bond with an electronegative atom in another or the same molecule. The third is the Carbon Hydrogen Bond formed between carbon and hydrogen. two of these bonds are formed and are shown in light green. As of 4th and 5th, there are Unfavorable Donor-Donor and Unfavorable acceptor-acceptor interactions. Pi cation hydrophobic interactions with Mg 2004 and Mg 3005 was also observed. In the 6th and 7th, one Pi-Pi Stacked and Covalent Bond were observed (**Figure 3-4-1**).

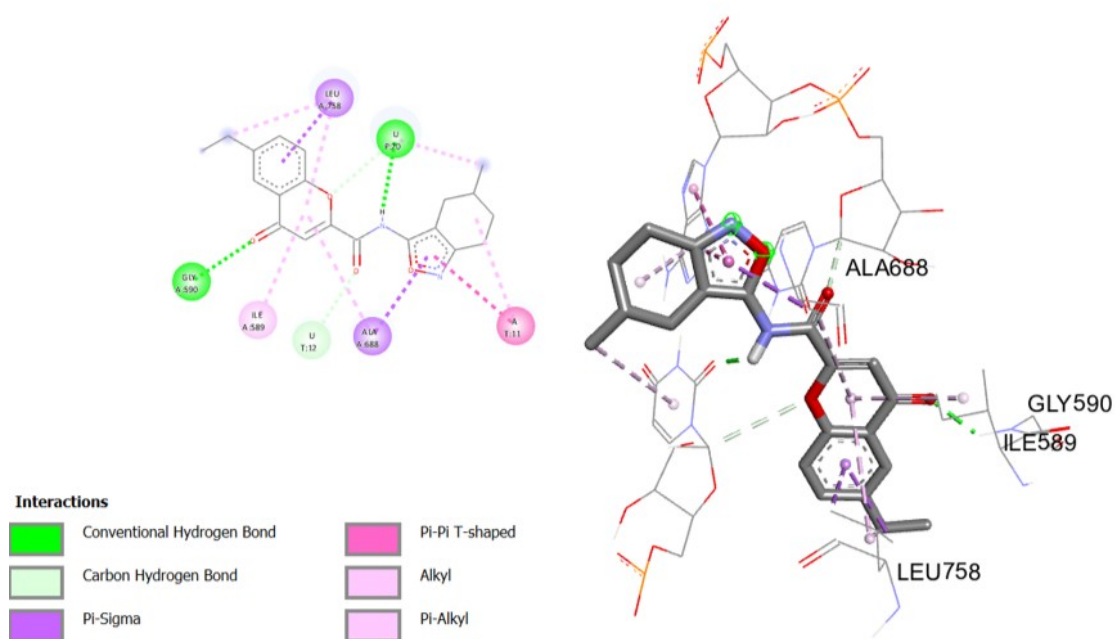


Figure 3-4-2 2D and 3D image of compound 7bv2 and Molecule1078(ligand).

The 2D and 3D shapes of the structure we created during the study can be seen in **Figure 3-4-2**. If we compare this shape with the crystallized form, all the bonds have changed. At first glance, the thing to say is that it has made less interaction. At the same time, no interaction is observed with POP and Mg. There are no undesirable links between interactions. While Conventional Hydrogen Bonds were on U (T:10) and U (P:20) in the original structure, there was an interaction between U (P:20) and GLY (A:590) in the new

docking structure. Comparing the Carbon Hydrogen Bond interaction, there are 2 interactions in the first build: they are Asp (A:760) and POP (A:1003). In the structure created with the Molecule 1078 ligand, it is U (T:12). Unlike the first structure, Pi-sigma ALA (A:688) and LEU (A:758) interactions occurred in the second structure. The overlap of frontier orbitals can occur with π and σ geometry, just like the overlap of atomic orbitals to produce molecular orbitals. Pi-pi T-shaped interaction that occurs in A (T:11) in the other interaction that occurs differently. This means: In a pi-pi T-shaped interaction, the pi-electron cloud interacts with the other aromatic groups in a T-shaped way, i.e., one ring's sidewise electron cloud interacts with the other rings head-on electron cloud. The other two interactions that occur are Alkyl and Pi-Alkyl interactions, and the regions where they occur are ILE (A:589), ALA (A:688), and LEU (A:758). No undesirable or problematic interaction was encountered in the resulting structure.

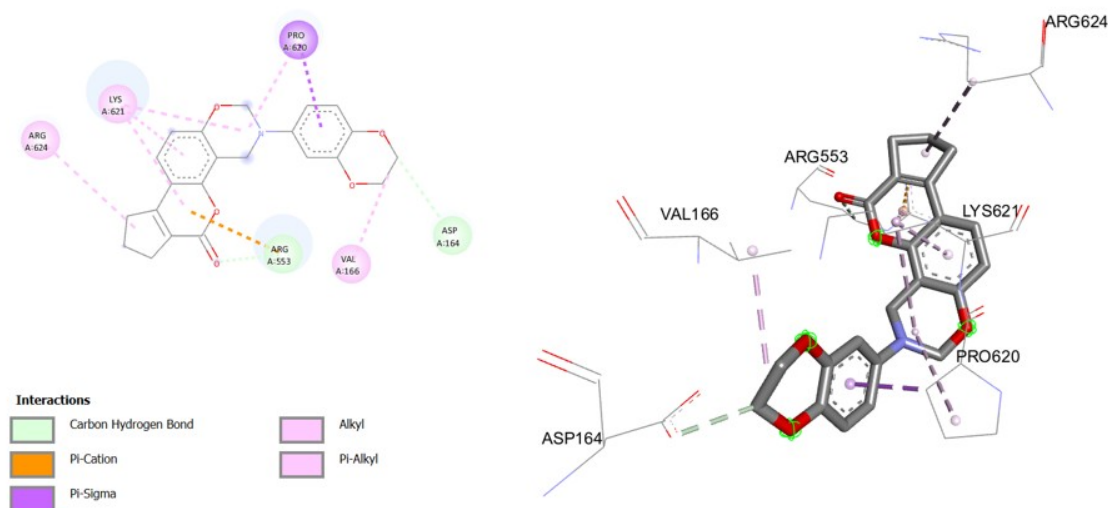


Figure 3-4-3 2D and 3D images of compounds 6m71 and Molecule618(ligand).

A 2D and 3D diagram was created for the other enzyme we used. No ligand was added while crystallizing in this enzyme. The A623 region, where the structure was combined with Remdesivir as the active site, was found and after docking studies between the ligands we received from OTAVA chemicals, it gave the best value with Molecule618. This structure, which gave the best value, was used while creating the model. As seen in **Figure 3-4-3**, 5 different interactions were observed between the ligand and the macromolecule. The first of these is the Carbon Hydrogen Bond interaction of ARG (A:553) and ASP (A:164) with the ligand. ARG (A:553) is also involved in Pi-cation

interaction. PRO (A:620), which creates Pi-Sigma interaction, also has two interactions like Arginine, in addition to the first interaction, Pi-alkyl interaction is also present. The last and most common interaction is the Alkyl interaction. VAL(A:166), LYS (A:621) interacted from 3 points, ARG(A:623).

3.5 NAMD Molecular Dynamic Simulation Results

After AutoDock-Vina, AutoDock4 scanning of the two enzymes and 1170 ligands used, it was decided to perform MD simulation for the enzyme and ligand with the lowest binding energy. Enzyme construct 7bv2 and ligand Molecule1078 were used to simulate MD. this compound was simulated with 50 ns production. The root mean square deviation (RMSD), the radius of rotation (Rg), mean square fluctuation (RMSF) profiles of the simulated system were calculated to see the values at which the complexes were stabilized. The inhibitor used remained bonded to the enzyme throughout the MD simulation. It has been observed that all inhibitors that inhibit the activity of enzymes and remain bound to the enzyme maintain their interactions.

3.5.1 Root Mean Square Deviation (RMSD)

Root mean square deviation graphs of the construct systems containing enzyme (7bv2) and best ligand (1078) are shown in *Figure 3-5-1*. While the generated system was running, it showed a steady state of equilibrium throughout the MD simulations. The RMSD of the 7bv2 enzyme and the Molecule1078 inhibitor TSN added to it increased slowly and steadily from $\sim 2\text{\AA}$ to $\sim 3.5\text{\AA}$ over the entire 50 ns of the MD study. There were no disconnections or splashes on the system. There was a slight fluctuation between 45 ns and 50 ns, and the energy of the system was $\sim 3\text{\AA}$ Decreased from A to $\sim 2.5\text{\AA}$.

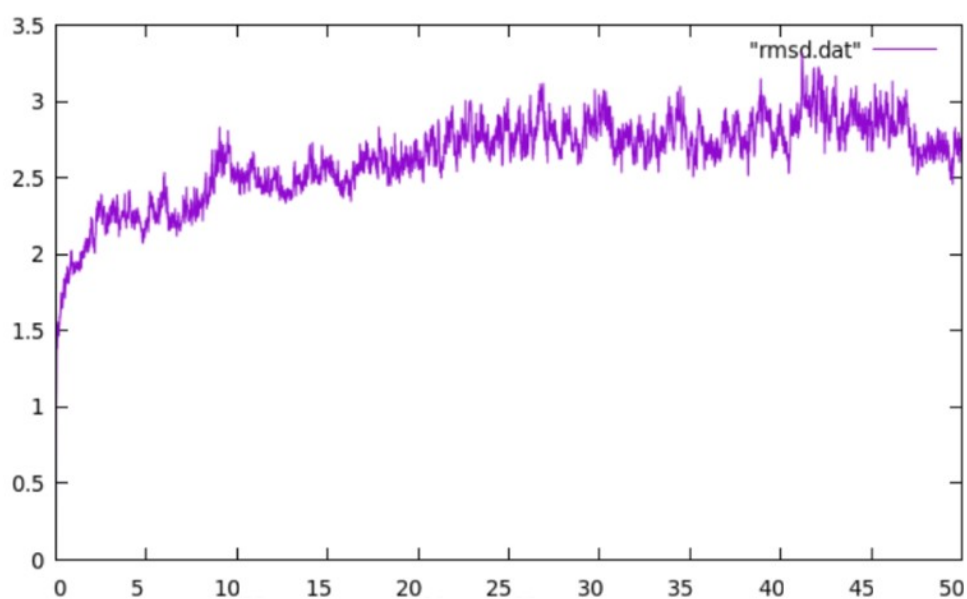


Figure 3-5-1 RMSD graphs of 7bv2 and Molecule1078 complex.

3.5.2 Root Mean Square Fluctuation (RMSF)

The mean square fluctuation (RMSF) analysis was performed for the complex system created and the results are shown *in Figure 3-5-2*. The fluctuations in the RMSF analysis can be explained by amino acid residues and their movements. When we look at the graph in Figure 3-5-2; peak areas and plateau areas are seen on the graph. The peaks in this graph are where the protein domains show the most fluctuation over the simulation time frame. The more peaking areas on the graph, the better inhibition of that ligand. Secondary structural elements such as alpha-helix parts and beta-sheet parts in the structure are generally more rigid than other parts of the protein and therefore fluctuate less than the loop regions. The graph created in this section has 3 main peaks and if it is evaluated with another complex, these peak points should be taken into account.

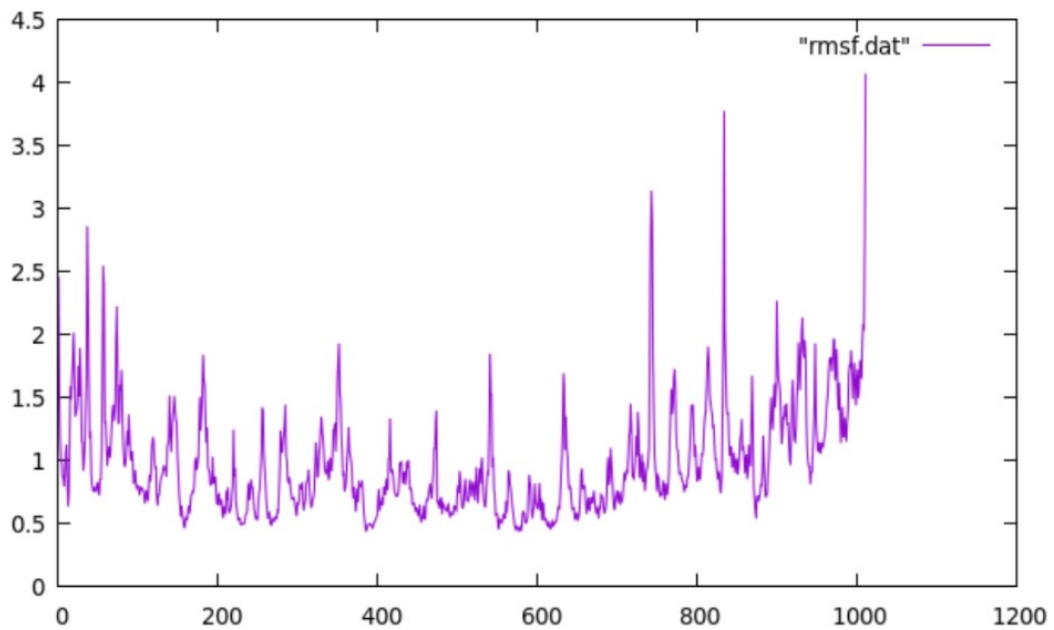


Figure 3-5-2 RMSF graphs of 7bv2 and Molecule1078 complex.

3.5.3 Radius of Gyration (Rg)

The radius of rotation (Rg) indicates the 3D structural stability and compactness of the protein structure. Here, it is observed that the Rg profile of the complex varies between ~35 Å and ~38 Å throughout the simulation (*Fig. 3-5-3*).

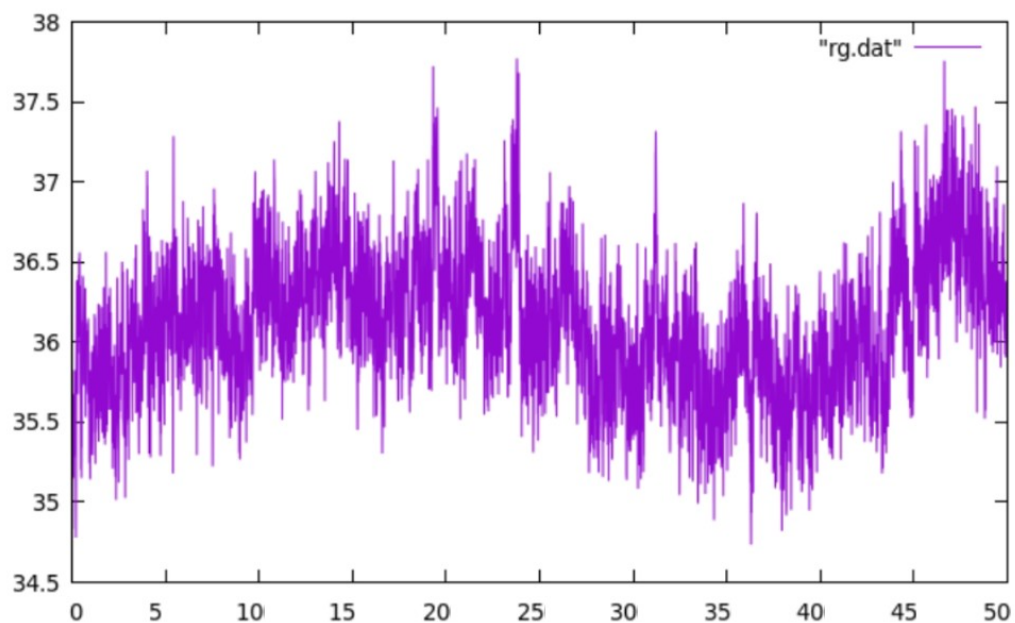


Figure 3-5-3 Rg graph of 7bv2 and Molecule1078 complex.

3.5.4 Potential Energy (PE)

The potential energy (PE) profile is the indicator that shows the total energy of the system and the physical validity of the simulation performed. The potential energy graph of the RdRp enzyme and Molecule1078 is shown in **Figure 3-5-4**. No power interruption was observed in the graph and also no fluctuation was observed. This means that the simulation is successful and balanced.

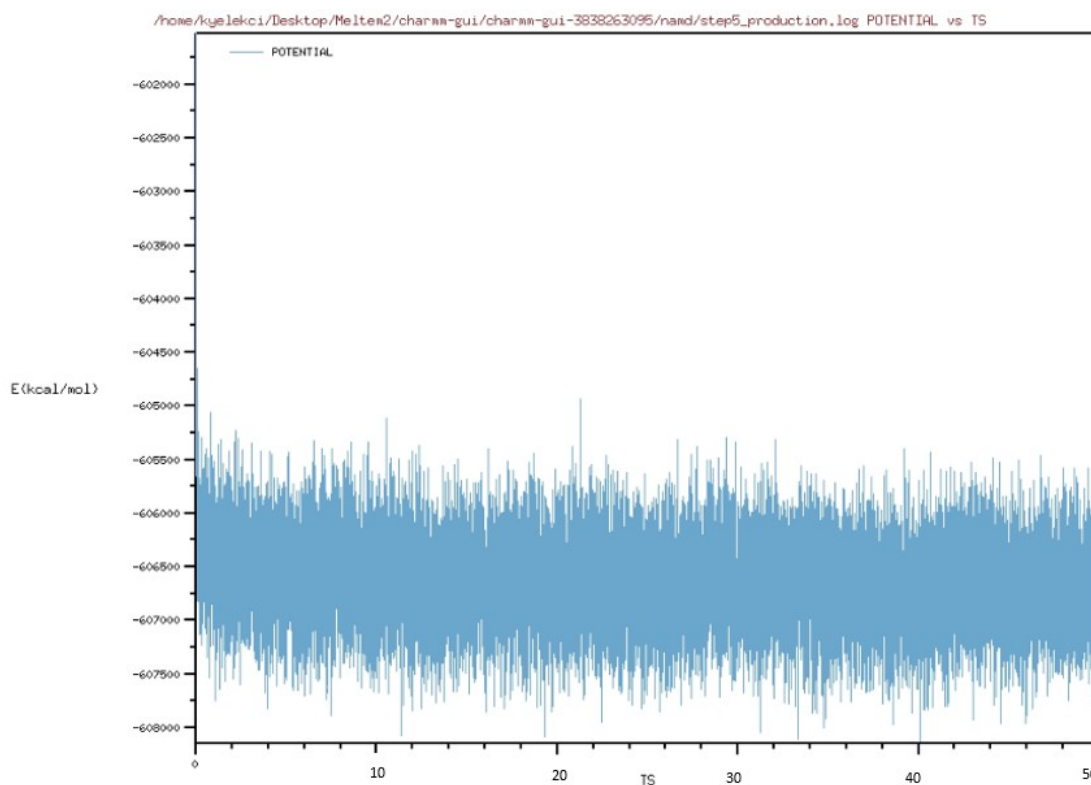


Figure 3-5-4 Potential Energy graph of 7bv2 and Molecule1078 complex.

4. CONCLUSION

More than one docking study was carried out in the study. After the first Autodock-Vina study yielded successful results, the first 5 molecules of both enzymes with the best n-binding energy were processed. For the 7bv2 enzyme, the result is Molecule798 > Molecule817 > Molecule1078 > Molecule302 > Molecule292. Molecule798: -8.5 showed the best binding energy. For the other enzyme 6m71, the order is as follows: Molecule373 > Molecule966 > Molecule1143 > Molecule321 > Molecule618. The best value is Molecule373: -9.0. These enzymes were also evaluated in the Autodock4 application to get more reliable and stable answers. as a result, for 7bv2: Molecule1078 > Molecule817 > Molecule798 > Molecule302 > Molecule292 result is like this. Molecule1078: -8.77 showed the best binding energy. For the other enzyme 6m71, the order is as follows: Molecule618 > Molecule 321 > Molecule373 > Molecule966 > Molecule1143. the best value is Molecule618: -8.13. The reason for the differences between the two operations is the different parameters used by the applications, and at the same time, the values may give different results on different computers. After the Autodock4 application, the interactions of the enzymes with the structures with the best properties were evaluated. No problem was observed. When the ADME study was performed for the top 10 selected models, it was concluded that all molecular structures conformed to ADME rules and all of them showed drug properties. In this study, the 7bv2 structure with the best binding energy and the Molecule1078 structure were evaluated, and this structure completed the ADME step without any problems and with good results. The structure is very successful in dissolving. Finally, the NAMD study was applied for this complex structure and the ligand molecule placed in the structure adapted to the structure and all the graphics created as a result of the NAMD process reached results that prove this. No situations such as energy disconnection, fluctuation, or lack of energy were encountered. The formed complex can be an inhibitor that can block the RdRp enzyme by fulfilling its drug-like structure and having low binding energy. As a result of the study, within the scope of all the data and results, the target was achieved with a successful result.

REFERENCES

- Anon n.d. *COVID-19: Finding the Right Fit Identifying Potential Treatments Using a Data-Driven Approach*. [online] Available at: <www.drugbankplus.com>.
- Aparoy, P., Reddy, K.K. and Reddanna, P., 2012. *Structure and Ligand Based Drug Design Strategies in the Development of Novel 5-LOX Inhibitors*. *Current Medicinal Chemistry*,
- Berlin, I., Thomas, D., le Faou, A.L. and Cornuz, J., 2020. *COVID-19 and smoking*. *Nicotine and Tobacco Research*, <https://doi.org/10.1093/ntr/ntaa059>.
- Boopathi, S., Poma, A.B. and Kolandaivel, P., 2020. *Novel 2019 coronavirus structure, mechanism of action, antiviral drug promises and rule out against its treatment*. *Journal of Biomolecular Structure and Dynamics*, <https://doi.org/10.1080/07391102.2020.1758788>.
- Carver, P.E. and Phillips, J., 2020. *Novel Coronavirus (COVID-19): What You Need to Know*. *Workplace Health and Safety*, <https://doi.org/10.1177/2165079920914947>.
- Chu, D.K., Pan, Y., Cheng, S.M., Hui, K.P., Krishnan, P., Liu, Y., Ng, D.Y., Wan, C.K., Yang, P., Wang, Q., Peiris, M. and Poon, L.L., 2020a. Abbreviations: TCID 50 Median tissue culture infectious dose; SARS-Severe Acute Respiratory Syndrome; MERS-Middle East Respiratory Syndrome. [online] <https://doi.org/10.1093/clinchem/hvaa029/5719336>.
- Chu, D.K., Pan, Y., Cheng, S.M., Hui, K.P., Krishnan, P., Liu, Y., Ng, D.Y., Wan, C.K., Yang, P., Wang, Q., Peiris, M. and Poon, L.L., 2020b. Abbreviations: TCID 50 Median tissue culture infectious dose; SARS-Severe Acute Respiratory Syndrome; MERS-Middle East Respiratory Syndrome. [online] <https://doi.org/10.1093/clinchem/hvaa029/5719336>.
- Daina, A., Michielin, O. and Zoete, V., 2017. SwissADME: A free web tool to evaluate pharmacokinetics, drug-likeness, and medicinal chemistry friendliness of small molecules. *Scientific Reports*, 7. <https://doi.org/10.1038/srep42717>.
- Di, L., 2015. Strategic Approaches to Optimizing Peptide ADME Properties. *AAPS Journal*, 17(1), pp.134–143. <https://doi.org/10.1208/s12248-014-9687-3>.
- Gao, Y., Yan, L., Huang, Y., Liu, F., Zhao, Y., Cao, L., Wang, T., Sun, Q., Ming, Z., Zhang, L., Ge, J., Zheng, L., Zhang, Y., Wang, H., Zhu, Y., Zhu, C., Hu, T., Hua, T., Zhang, B., Yang, X., Li, J., Yang, H., Liu, Z., Xu, W., Guddat, L.W., Wang, Q., Lou, Z. and Rao, Z., 2020. Structure of the RNA-dependent RNA polymerase from COVID-19 virus. *Science*, 368(6492), pp.779–782. <https://doi.org/10.1126/science.abb7498>.
- van Hemert, M.J., van den Worm, S.H.E., Knoops, K., Mommaas, A.M., Gorbalenya, A.E. and Snijder, E.J., 2008. SARS-coronavirus replication/transcription complexes are membrane-protected and need a host factor for activity in vitro. *PLoS Pathogens*, 4(5). <https://doi.org/10.1371/journal.ppat.1000054>.
- Karamertzanis, P.G. and Price, S.L., 2006. Energy minimization of crystal structures containing flexible molecules. *Journal of Chemical Theory and Computation*, 2(4), pp.1184–1199. <https://doi.org/10.1021/ct600111s>.

- Kim, S., Lee, J., Jo, S., Brooks, C.L., Lee, H.S. and Im, W., 2017. CHARMM-GUI ligand reader and modeler for CHARMM force field generation of small molecules. *Journal of Computational Chemistry*, 38(21), pp.1879–1886. <https://doi.org/10.1002/jcc.24829>.
- Kirchdoerfer, R.N., Cottrell, C.A., Wang, N., Pallesen, J., Yassine, H.M., Turner, H.L., Corbett, K.S., Graham, B.S., McLellan, J.S. and Ward, A.B., 2016. Pre-fusion structure of a human coronavirus spike protein. *Nature*, 531(7592), pp.118–121. <https://doi.org/10.1038/nature17200>.
- Kumar, K. and Lupoli, T.J., 2020. *Exploiting Existing Molecular Scaffolds for Long-Term COVID Treatment*. *ACS Medicinal Chemistry Letters*, <https://doi.org/10.1021/acsmchemlett.0c00254>.
- Kumar, V., Doshi, K.U., Khan, W.H. and Rathore, A.S., 2021. COVID-19 pandemic: mechanism, diagnosis, and treatment. *Journal of Chemical Technology and Biotechnology*, 96(2), pp.299–308. <https://doi.org/10.1002/jctb.6641>.
- Lipinski, C.A., 2004. *Lead- and drug-like compounds: The rule-of-five revolution*. *Drug Discovery Today: Technologies*, <https://doi.org/10.1016/j.ddtec.2004.11.007>.
- Meng, X.-Y., Zhang, H.-X., Mezei, M. and Cui, M., n.d. *Molecular Docking: A powerful approach for structure-based drug discovery*.
- Morris, G.M., Goodsell, D.S., Pique, M.E., Huey, R., Forli, S., Hart, W.E., Halliday, S., Belew, R., and Olson, A.J., 1991. *User Guide AutoDock Version 4.2 Updated for version 4.2.6 Automated Docking of Flexible Ligands to Flexible Receptors*. [online] Available at: <<http://autodock.scripps.edu/>>.
- Pardo, J., Shukla, A.M., Chamarthi, G., and Gupte, A., 2020. *The journey of remdesivir: From Ebola to COVID-19*. *Drugs in Context*, <https://doi.org/10.7573/DIC.2020-4-14>.
- Pardridge, W.M., n.d. *The Blood-Brain Barrier: Bottleneck in Brain Drug Development*.
- Pastick, K.A., Okafor, E.C., Wang, F., Lofgren, S.M., Skipper, C.P., Nicol, M.R., Pullen, M.F., Rajasingham, R., McDonald, E.G., Lee, T.C., Schwartz, I.S., Kelly, L.E., Lother, S.A., Mitjà, O., Letang, E., Abassi, M. and Boulware, D.R., 2020. *Review: Hydroxychloroquine and chloroquine for treatment of SARS-CoV-2 (COVID-19)*. *Open Forum Infectious Diseases*, <https://doi.org/10.1093/ofid/ofaa130>.
- Phillips, J.C., Braun, R., Wang, W., Gumbart, J., Tajkhorshid, E., Villa, E., Chipot, C., Skeel, R.D., Kalé, L. and Schulten, K., 2005. *Scalable molecular dynamics with NAMD*. *Journal of Computational Chemistry*, <https://doi.org/10.1002/jcc.20289>.
- Pilkington, V., Pepperrell, T. and Hill, A., 2020. *A review of the safety of favipiravir—a potential treatment in the COVID-19 pandemic?* *Journal of Virus Eradication*, .
- Popa, I., Gillies, G., Papastavrou, G. and Borkovec, M., 2010. Attractive and repulsive electrostatic forces between positively charged latex particles in the presence of anionic linear polyelectrolytes. *Journal of Physical Chemistry B*, 114(9), pp.3170–3177. <https://doi.org/10.1021/jp911482a>.

- Shu, B. and Gong, P., 2016. Structural basis of viral RNA-dependent RNA polymerase catalysis and translocation. *Proceedings of the National Academy of Sciences of the United States of America*, 113(28), pp.E4005–E4014. <https://doi.org/10.1073/pnas.1602591113>.
- Shweta, M., Rashmi, D. and Mishra, S., 2011. In-vitro ADME studies of TUG-891, a GPR-120 inhibitor using Swiss ADME predictor. [online] <https://doi.org/10.22270/jddt.v9i2-s.2710>.
- Simmons, G., Gosalia, D.N., Rennekamp, A.J., Reeves, J.D., Diamond, S.L. and Bates, P., 2005. *Inhibitors of cathepsin L prevent severe acute respiratory syndrome coronavirus entry*. [online] Available at: <www.pnas.org/cgi/doi/10.1073/pnas.0505577102>.
- Trott, O. and Olson, A.J., 2009. AutoDock Vina: Improving the speed and accuracy of docking with a new scoring function, efficient optimization, and multithreading. *Journal of Computational Chemistry*, p.NA-NA. <https://doi.org/10.1002/jcc.21334>.
- Wilson, G.L. and Lill, M.A., 2011. *Integrating structure-based and ligand-based approaches for computational drug design*. *Future Medicinal Chemistry*, <https://doi.org/10.4155/fmc.11.18>.
- Yin, W., Mao, C., Luan, X., Shen, D.-D., Shen, Q., Su, H., Wang, X., Zhou, F., Zhao, W., Gao, M., Chang, S., Xie, Y.-C., Tian, G., Jiang, H.-W., Tao, S.-C., Shen, J., Jiang, Y., Jiang, H., Xu, Y., Zhang, S., Zhang, Y. and Xu, H.E., n.d. *Structural basis for inhibition of the RNA-dependent RNA polymerase from SARS-CoV-2 by remdesivir*.
- Yüce, M., Filiztekin, E. and Özkaya, K.G., 2021. COVID-19 diagnosis —A review of current methods. *Biosensors and Bioelectronics*, 172. <https://doi.org/10.1016/j.bios.2020.112752>.
- Centers for Disease Control and Prevention, 2021. *Symptoms of COVID-19*. [Online] Available at: <https://www.cdc.gov/coronavirus/2019-ncov/symptoms-testing/symptoms.html> [Accessed December 2021].
- Centers for Disease Control and Prevention, 2021. *Symptoms of COVID-19*. [Online] Available at: <https://www.cdc.gov/coronavirus/2019-ncov/symptoms-testing/symptoms.html> [Accessed December 2021].
- Giuseppe Pascarella, A. S. C. P. F. B. R. D. B. F. S. S. & F. E. A., 2020. *Wiley*. [Online] Available at: <https://onlinelibrary.wiley.com/doi/epdf/10.1111/joim.13091> [Accessed December 2021].
- invivogen.com, n.d. *remdesivir*. [Online] Available at: <https://www.invivogen.com/remdesivir> [Accessed 2021].
- OTAVA chemicals, n.d. *SARS-CoV-2 Helicase Targeted Library*. [Online] Available at: https://www.otavachemicals.com/products/targeted-libraries-and-focused-libraries/sars-cov-2/sars-cov-2-helicase-targeted-library?utm_medium=email&utm_source=UniSender&utm_campaign=2371796

[Accessed December 2021].

- US FDA, 2020. *Hydroxychloroquine or Chloroquine for COVID-19*. [Online] Available at: <https://www.fda.gov/safety/medical-product-safety-information/hydroxychloroquine-or-chloroquine-covid-19-drug-safety-communication-fda-cautions-against-use> [Accessed 2021].
- World Health Organization, 2019. *Coronavirus disease (COVID-19) pandemic*. [Online] Available at: <https://www.who.int/emergencies/diseases/novel-coronavirus-2019> [Accessed 10 december 2021].
- Worldometer, 2021. *COVID-19 CORONAVIRUS PANDEMIC*. [Online] Available at: <https://www.worldometers.info/coronavirus/> [Accessed 12 December 2021].

CURRICULUM VITAE

Personal Information

Name Surname :Meltem YILDIRIM

Education

Undergraduate Education: **Kadir Has University**

Bioinformatic and Genetic Department

Graduate Education: **Kadir Has University**

Computational Biolog and Bioinformatic

Languages : English: Reading: Advanced, Writing: Advanced, Speaking:
Advanced

Germany Reading: Beginner, Writing: Beginner, Speaking:
Beginner

Turkish: native

Work / Internship Experience

07/2017 – 08/2017: İstanbul University Capa Medical School Hospital

Department Medical Biology, Tissue Lab

Survey to genetic diseases using DNA analysis with NGS SSO, SSP, Facs Flow, and similar techniques. Sanger Sequencing. DNA isolation. Sampling

06/2018 – 07/2018: İbrahim Etem – Menarini Group

Department Microbiology,

Sample registration and acceptance. Membrane preparation. Non- sterile gloves analysis. Gram coloring. Quantity measurement. B.E.T analysis for injection water. Bioburden (Biological Load Quantity Test) analysis. Sealing test. Api test. Syrup analysis. Tablet analysis. Environmental control. Kinetic turbidimetric analysis for detecting bacteria

ADDITIONAL EDUCATION & CERTIFICATES

07/09/2016 International Molecular Biology and Genetic Student Congress

Gene Therapy, Personalized Medicine, Neuroscience

Epigenetics, Synthetic Biology, Development Biology

29/01/2018 Evolutionary Genomics winter school

06/05/2019 Best Designed Project (Kadir Has Uni): New Acetylcholinesterase Inhibitors for Alzheimer

07/03/2020 Medical Biotechnology Congress

Computer Skills

Word, Excel, Powerpoint, Outlook: Excellent VMD: Excellent

AutoDock: Excellent

PyMOL: Excellent

BIOVIA: Excellent

R studio: Good

Unix: Excellent

Python: Excellent

MATLAB: Good

Mgltools: Excellent

VMD: Excellent